

On SYK traversable wormhole with imperfectly correlated disorders

Tomoki Nosaka^{*1} and Tokiro Numasawa^{†2}

¹: *Kavli Institute for Theoretical Sciences, University of Chinese Academy of Sciences, Beijing, China 100190*

²: *Institute for Solid State Physics, University of Tokyo, Kashiwa 277-8581, Japan*

Abstract

In this paper we study the phase structure of two Sachdev-Ye-Kitaev models (L -system and R -system) coupled by a simple interaction, with imperfectly correlated disorder. When the disorder of the two systems are perfectly correlated, $J_{i_1 \dots i_q}^{(L)} = J_{i_1 \dots i_q}^{(R)}$, this model is known to exhibit a phase transition at a finite temperature between the two-black hole phase at high-temperature and the traversable wormhole phase at low temperature. We find that, as the correlation $\langle J_{i_1 \dots i_q}^{(L)} J_{i_1 \dots i_q}^{(R)} \rangle$ is decreased, the critical temperature becomes lower. At the same time, the transmission between L -system and R -system in the low-temperature phase becomes more suppressed, while the chaos exponent of the whole system becomes larger. Interestingly we also observe that when the correlation is smaller than some q -dependent critical value the phase transition completely disappears in the entire parameter space. At zero temperature, the energy gap becomes larger as we decrease the correlation. We also use a generalized thermofield double state as a variational state. Interestingly, this state coincide with the ground state in the large q limit.

^{*}nosaka@yukawa.kyoto-u.ac.jp

[†]numasawa@issp.u-tokyo.ac.jp

Contents

| | | |
|----------|--|-----------|
| 1 | Introduction and Summary | 2 |
| 2 | $J_{i_1 \dots i_q}^{(L)} \neq J_{i_1 \dots i_q}^{(R)}$ model | 4 |
| 3 | Finite q, large N | 8 |
| 3.1 | Phase diagram | 8 |
| 3.2 | Energy gap | 13 |
| 3.3 | Real time response | 14 |
| 3.3.1 | Transmission amplitude in low temperature regime | 15 |
| 3.3.2 | Chaos exponent | 15 |
| 4 | large q limit | 19 |
| 4.1 | large q limit at zero temperature | 19 |
| 4.2 | Finite temperature | 22 |
| 4.3 | Absence of phase transitions for small $\tilde{\mathcal{J}}/\mathcal{J}$ | 26 |
| 4.4 | Inverse temperature of order $\beta \sim q$ and beyond | 28 |
| 4.4.1 | Comments on subleading Lyapunov exponents | 29 |
| 5 | Structure of ground state for imperfectly correlated disorders | 29 |
| 5.1 | Variational approximation in large q limit | 30 |
| 5.2 | Overlap between ground state and $ I(\beta)\rangle$ for finite q | 32 |
| 6 | Discussion and Future works | 33 |
| A | A derivation of the large q partition function | 36 |
| B | Relation between ground state of H_{int} and eigenstates of $H_{SYK}^{(a)}$ | 37 |
| B.1 | Gamma matrices and charge conjugation matrix | 38 |
| B.2 | $q = 0 \bmod 4$ | 39 |
| B.2.1 | $q = 0 \bmod 4$, $N = 0 \bmod 8$ | 39 |

| | | |
|-------|-----------------------------------|----|
| B.2.2 | $q = 0 \bmod 4, N = 2, 6 \bmod 8$ | 40 |
| B.2.3 | $q = 0 \bmod 4, N = 4 \bmod 8$ | 41 |
| B.3 | $q = 2 \bmod 4$ | 42 |
| B.3.1 | $q = 2 \bmod 4, N = 0, 4 \bmod 8$ | 42 |
| B.3.2 | $q = 2 \bmod 4, N = 2, 6 \bmod 8$ | 43 |

1 Introduction and Summary

The Sachdev-Ye-Kitaev (SYK) model [1, 2] is a useful model to study various aspects of strongly coupled many body systems. Moreover, the SYK model is also a toy model of quantum black hole [3]. Both theories show the same pattern of the conformal symmetry breaking at low energy and described by the so-called Schwarzian action. This gives a concrete connection between two theories.

Related to black holes, the SYK model also plays an important role to understand wormhole configurations in gravity. Two kind of wormholes play important roles in the literature. The first one is the spacial wormhole. Spacial wormholes are related to entanglement [4, 5, 6]. In the context of AdS/CFT correspondence, the area of the wormhole connecting distant regions corresponds to entanglement entropy in CFT [7, 8, 9]. Moreover, it is expected that spacial wormholes are dual to entanglement between CFTs [5, 6] and the spacetime is built from entanglement [10, 11]. The other kind of wormhole is the spacetime wormholes or Euclidean wormholes. These are kinds of gravitational instanton and these spacetime wormholes are related to random couplings [12, 13, 14]. The SYK model is a model with random couplings and the wormhole configurations associated to a pattern of random couplings are studied [15, 16]. These Euclidean wormholes also appears in the context of calculation of (Rényi) entanglement entropy. These are known as replica wormholes [17, 18] and play important roles in the context of black hole information problems.

Usually we assume that the random couplings of copies of SYK models have exactly the same couplings, i.e. in each realization of the random couplings we use the same realization for all of the copies. This is natural setup when we use the replica methods to study the Rényi entropy for example. However, to study entangled states we can also consider the situation where the copies of SYK models have different random couplings. For example, if we simulate the SYK models on quantum computers it maybe natural to consider different realization because of errors etc. Furthermore, we can also consider entangled black holes between different theories.

For example, “Janus black holes”, i.e., two side black holes that are dual to entangled state with different coupling constants, are studied in [19, 20, 21, 22, 23].

Motivated by the above questions, we study the coupled SYK models where the two SYK models have different realization of random couplings. The two-coupled SYK model was first considered in [24], with the two random couplings perfectly correlated, as the holographic dual of the global AdS_2 spacetime (eternal traversable wormhole), which is the static version of the wormhole formation process by the bulk non-local interaction [25, 3]. In the setup of [24], in order the wormhole to become traversable, or in the SYK side the quantum teleportation to be successful, it is crucial for the state of the whole system to be the thermofield double state [26]. It was found that the ground state of the coupled SYK model is close to the thermofield double state [24, 27, 28], which ensures that the low temperature dynamics of the model can be related to the traversable wormhole. Indeed, the coupled SYK model in the canonical ensemble exhibits a Hawking-Page-like phase transition between the high temperature phase dual to the two-sided AdS_2 black hole and the low temperature phase dual to the global AdS_2 .

When the couplings of the two systems are different, it is not clear how to interpret the entanglement structure of the ground state and whether the system is dual to the traversable wormhole at low temperature or not. It was also found in [29, 30] that the coupled SYK model does not exhibit a phase transition when the two random couplings are completely independent. Hence the correlation of the couplings is indeed important for the wormhole formation, and it is a non-trivial question how much correlation would be necessary for the wormhole to be formed.

More concretely, we consider the model where the two random couplings $J_{i_1 \dots i_q}^{(L)}$ and $J_{i_1 \dots i_q}^{(R)}$ obey the same Gaussian distribution while the two realizations are not completely identical, which we quantify by $\langle J_{i_1 \dots i_q}^{(L)} J_{i_1 \dots i_q}^{(R)} \rangle$ normalized by $\langle (J_{i_1 \dots i_q}^{(L)})^2 \rangle (= \langle (J_{i_1 \dots i_q}^{(R)})^2 \rangle)$. By analyzing this model in the large N limit, we find the following results:

- (i) As the correlation between the two random couplings is decreased, the critical temperature for the Hawking-Page-like phase transition becomes lower. This result can also be rephrased that the strength of the LR coupling required for reaching the wormhole phase at fixed temperature becomes higher, hence both the correlation of random couplings and direct LR coupling make it easy to create a wormhole configuration. This is also consistent with the fact that the wormhole phase exists even without direct LR coupling if the two random couplings are *superrelated*, $\langle J_{i_1 \dots i_q}^{(L)} J_{i_1 \dots i_q}^{(R)} \rangle > \langle (J_{i_1 \dots i_q}^{(L)})^2 \rangle$ [31, 32, 33, 34, 35].
- (ii) We also observe that the phase transition completely disappears when the correlation between $J_{i_1 \dots i_q}^{(L)}$ and $J_{i_1 \dots i_q}^{(R)}$ is smaller than some non-zero finite value. Technically this occurs in the following way. Already in the original setup where the two random couplings are identical, there are no phase transition when the LR coupling is larger than some

critical value: when the LR coupling is too large, even at a high temperature the dynamics is approximately same as that for the model without SYK interaction which does not exhibit phase transition. We find that this critical value of the LR coupling becomes smaller as the correlation between $J_{i_1 \dots i_q}^{(L)}$ and $J_{i_1 \dots i_q}^{(R)}$ is decreased, and reaches zero before the two random coupling become completely independent. At large q limit, we also estimate when the phase transition disappears as we decrease the correlation of random couplings between two sides.

- (iii) We also evaluate the transmission amplitude T_{LR} between the L -site and the R -site in the low temperature wormhole phase, and found that for the same temperature and the strength of the LR coupling, T_{LR} becomes smaller as the correlation between $J_{i_1 \dots i_q}^{(L)}$ and $J_{i_1 \dots i_q}^{(R)}$ is decreased. On the other hand, the chaos exponent λ_L , which is non-zero even in the wormhole phase, becomes larger as the correlation of the random couplings is decreased. These two results are reasonable if λ_L of this model measures the speed that a simple initial excitation spread within single site, which would be suppressed if the excitation leaks to the other site.

We observe the results (i-iii) numerically for $q = 4$, and also confirm the results (i,ii) analytically in the large q limit.

The organization of this paper is as follows. In section 2, we clarify the model we study in this paper, and write the partition function in the large N limit with the bilocal field formalism. By using the bilocal field formalism, we analyze how the large N phase structure and various properties of each phases are modified by the imperfect correlation of disorders for finite q in section 3 and in the large q limit in section 4. In section 5 we study the structure of the ground state of the coupled system for $\langle J_{i_1 \dots i_q}^{(L)} J_{i_1 \dots i_q}^{(R)} \rangle < \langle (J_{i_1 \dots i_q}^{(L)})^2 \rangle$ which generalizes the structure of the thermofield double state for $J_{i_1 \dots i_q}^{(L)} = J_{i_1 \dots i_q}^{(R)}$. In section 6 we summarize the our results and list possible future directions of research. Some technical details of the calculation in the large q limit are collected in appendix A.

2 $J_{i_1 \dots i_q}^{(L)} \neq J_{i_1 \dots i_q}^{(R)}$ model

In this paper we consider a one-dimensional quantum mechanics with the following disordered Hamiltonian:

$$H = H_{SYK}^{(L)} + H_{SYK}^{(R)} + \mu H_{int}, \quad (2.1)$$

where

$$\begin{aligned}
H_{SYK}^{(L)} &= i^{\frac{q}{2}} \sum_{i_1 < i_2 < \dots < i_q}^N J_{i_1 i_2 \dots i_q}^{(L)} \psi_{i_1}^L \psi_{i_2}^L \dots \psi_{i_q}^L, & H_{SYK}^{(R)} &= i^{\frac{q}{2}} (-1)^{\frac{q}{2}} \sum_{i_1 < i_2 < \dots < i_q}^N J_{i_1 i_2 \dots i_q}^{(R)} \psi_{i_1}^R \psi_{i_2}^R \dots \psi_{i_q}^R, \\
H_{int} &= i \sum_{i=1}^N \psi_i^L \psi_i^R,
\end{aligned} \tag{2.2}$$

$\{\psi_i^a, \psi_j^b\} = \delta_{ab} \delta_{ij}$ ($a = L, R$), and $J_{i_1 i_2 \dots i_q}^{(a)}$ are random couplings drawn from the Gaussian distribution with the following mean and variance:

$$\langle J_{i_1 i_2 \dots i_q}^{(a)} \rangle = 0, \quad \langle J_{i_1 i_2 \dots i_q}^{(a)} J_{j_1 j_2 \dots j_q}^{(a)} \rangle = \frac{\mathcal{J}^2 \cdot 2^{q-1} (q-1)!}{q \cdot N^{q-1}} \delta_{i_1 j_1} \delta_{i_2 j_2} \dots \delta_{i_q j_q}. \tag{2.3}$$

Here $J_{i_1 i_2 \dots i_q}^{(a)}$ are drawn independently for different set of subscripts $i_1 i_2 \dots i_q$. On the other hand, with respect to $a = L, R$, we consider the case where $J_{i_1 i_2 \dots i_q}^{(L)}$ and $J_{i_1 i_2 \dots i_q}^{(R)}$ are imperfectly correlated with each other:

$$\langle J_{i_1 i_2 \dots i_q}^{(L)} J_{j_1 j_2 \dots j_q}^{(R)} \rangle = \frac{\tilde{\mathcal{J}}^2 \cdot 2^{q-1} (q-1)!}{q \cdot N^{q-1}} \delta_{i_1 j_1} \delta_{i_2 j_2} \dots \delta_{i_q j_q}, \tag{2.4}$$

with $0 \leq \tilde{\mathcal{J}} \leq \mathcal{J}$.¹ This partial correlation can be realized by drawing two independent random variables $J_{i_1 i_2 \dots i_q}^{(\alpha)}$ ($\alpha = 1, 2$) from the same distribution as $J_{i_1 i_2 \dots i_q}^{(L)}$ (2.3) and writing $J_{i_1 i_2 \dots i_q}^{(a)}$ as

$$\begin{aligned}
J_{i_1 i_2 \dots i_q}^{(L)} &= J_{i_1 i_2 \dots i_q}^{(1)} \sqrt{\frac{1 + \tilde{\mathcal{J}}^2 / \mathcal{J}^2}{2}} + J_{i_1 i_2 \dots i_q}^{(2)} \sqrt{\frac{1 - \tilde{\mathcal{J}}^2 / \mathcal{J}^2}{2}}, \\
J_{i_1 i_2 \dots i_q}^{(R)} &= J_{i_1 i_2 \dots i_q}^{(1)} \sqrt{\frac{1 + \tilde{\mathcal{J}}^2 / \mathcal{J}^2}{2}} - J_{i_1 i_2 \dots i_q}^{(2)} \sqrt{\frac{1 - \tilde{\mathcal{J}}^2 / \mathcal{J}^2}{2}}.
\end{aligned} \tag{2.5}$$

Consider the Euclidean partition function (annealed average) of this theory at finite temperature β^{-1} :

$$\begin{aligned}
Z(\beta) &= \left\langle \int \mathcal{D}\psi_i^{(a)}(\tau) \exp \left[- \int d\tau \left(\sum_{a=L,R} \sum_{i=1}^N \frac{1}{2} \psi_i^a \partial_\tau \psi_i^a + H \right) \right] \right\rangle_{J_{i_1 i_2 \dots i_q}^{(\alpha)}} \\
&= \mathcal{N}^{-1} \int \left(\prod_{\alpha=1,2} \prod_{i_1 < i_2 < \dots < i_q}^N dJ_{i_1 i_2 \dots i_q}^{(\alpha)} e^{-\frac{1}{2} \frac{q \cdot N^{q-1}}{\mathcal{J}^2 \cdot 2^{q-1} (q-1)!} (J_{i_1 i_2 \dots i_q}^{(\alpha)})^2} \right) \\
&\quad \int \mathcal{D}\psi_i^{(a)}(\tau) \exp \left[- \int d\tau \left(\sum_{a=L,R} \sum_{i=1}^N \frac{1}{2} \psi_i^a \partial_\tau \psi_i^a + H \right) \right].
\end{aligned} \tag{2.6}$$

¹One may also consider the case $\tilde{\mathcal{J}} > \mathcal{J}$, where the Hamiltonian is non-Hermitian [31, 32, 33, 34, 35].

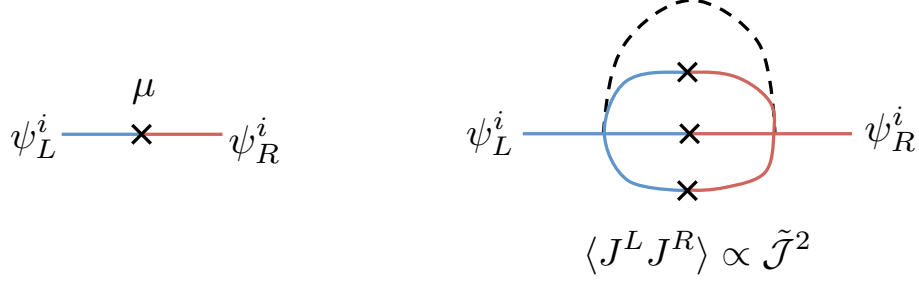


Figure 1: **Left:** A diagram that is not affected by the random couplings. **Right:** A typical diagram that is reduced when we decrease the correlation of left and right random couplings.

After the same manipulation as [30] we can rewrite the partition function in terms of the bilocal fields $G_{ab}(\tau, \tau')$ and $\Sigma_{ab}(\tau, \tau')$ as

$$Z(\beta) = \int \mathcal{D}G_{ab}(\tau, \tau') \mathcal{D}\Sigma_{ab}(\tau, \tau') e^{-S_E}. \quad (2.7)$$

The effective action is

$$\begin{aligned} -S_E/N = & \log \text{Pf} \left(-\delta(\tau - \tau') \partial_{\tau'} \delta_{ab} + \frac{\Sigma_{ab}(\tau, \tau') - \Sigma_{ba}(\tau', \tau)}{2} \right) \\ & - \frac{1}{2} \int d\tau d\tau' \sum_{a,b} \left[\Sigma_{ab}(\tau, \tau') G_{ab}(\tau, \tau') - s_{ab} \frac{\mathcal{J}_{ab}^2}{2q^2} [2G_{ab}(\tau, \tau')]^q \right] \\ & + \frac{i\mu}{2} \int d\tau [-G_{LR}(\tau, \tau) + G_{RL}(\tau, \tau)]. \end{aligned} \quad (2.8)$$

Here $s_{LL} = s_{RR} = 1$, $s_{LR} = s_{RL} = (-1)^{\frac{q}{2}}$ and $\mathcal{J}_{LL} = \mathcal{J}_{RR} = \mathcal{J}$, $\mathcal{J}_{LR} = \mathcal{J}_{RL} = \tilde{\mathcal{J}}$. The Schwinger-Dyson equations $\frac{\delta S_E}{\delta G_{ab}(\tau, \tau')} = \frac{\delta S_E}{\delta \Sigma_{ab}(\tau, \tau')} = 0$ are

$$\begin{aligned} \partial_{\tau} G_{ab}(\tau, \tau') - \sum_c \int d\tau'' \frac{\Sigma_{ac}(\tau, \tau'') - \Sigma_{ca}(\tau'', \tau)}{2} G_{cb}(\tau'', \tau') &= \delta_{ab} \delta(\tau - \tau'), \\ \Sigma_{ab}(\tau, \tau') &= \frac{s_{ab} \mathcal{J}_{ab}^2}{q} (2G_{ab}(\tau, \tau'))^{q-1} + i\mu (-\delta_{aL} \delta_{bR} + \delta_{aR} \delta_{bL}) \delta(\tau - \tau'). \end{aligned} \quad (2.9)$$

From the two equations it follows that

$$G_{ab}(\tau, \tau') = -G_{ba}(\tau', \tau). \quad (2.10)$$

By identifying $G_{ab}(\tau, \tau')$ with $(\alpha = 1, 2)$

$$G_{ab}(\tau, \tau') = \frac{1}{N} \sum_{i=1}^N \langle \mathcal{T} \psi_i^a(\tau) \psi_i^b(\tau') \rangle_{\beta} \quad (2.11)$$

$$= \begin{cases} \frac{1}{N \langle \text{tr} e^{-\beta H} \rangle_{J_{i_1 \dots i_q}^{(\alpha)}}} \sum_{i=1}^N \langle \text{tr} e^{\tau H} \psi_i^a e^{-H(\tau-\tau')} \psi_i^b e^{-(\tau'+\beta)H} \rangle_{J_{i_1 \dots i_q}^{(\alpha)}}, & (\tau > \tau') \\ -\frac{1}{N \langle \text{tr} e^{-\beta H} \rangle_{J_{i_1 \dots i_q}^{(\alpha)}}} \sum_{i=1}^N \langle \text{tr} e^{\tau' H} \psi_i^b e^{-H(\tau'-\tau)} \psi_i^a e^{-(\tau+\beta)H} \rangle_{J_{i_1 \dots i_q}^{(\alpha)}}, & (\tau < \tau') \end{cases}, \quad (2.12)$$

we also find that $G_{ab}(\tau, \tau')$ obeys the following conditions ²

$$G_{ab}(\tau, \tau')^* = -G_{ab}(-\tau, -\tau'), \quad G_{ab}(\tau + \beta, \tau') = -G_{ab}(\tau, \tau'). \quad (2.13)$$

From (2.12) and (2.9) it also follows that $G_{ab}(\tau, \tau'), \Sigma_{ab}(\tau, \tau')$ depends on τ, τ' only through $\tau - \tau'$, hence we may denote $G_{ab}(\tau, \tau')$ and $\Sigma_{ab}(\tau, \tau')$ respectively as $G_{ab}(\tau - \tau'), \Sigma_{ab}(\tau - \tau')$. Taking these into account, the Schwinger-Dyson equations (2.9) and the symmetry properties (2.10), (2.13) are written in a simpler way as

$$\begin{aligned} \partial_\tau G_{ab}(\tau) - \sum_c \int d\tau' \Sigma_{ac}(\tau - \tau') G_{cb}(\tau') &= \delta_{ab} \delta(\tau), \\ \Sigma_{ab}(\tau) &= \frac{s_{ab} \mathcal{J}_{ab}^2}{q} (2G_{ab}(\tau))^{q-1} + i\mu(-\delta_{aL}\delta_{bR} + \delta_{aR}\delta_{bL})\delta(\tau), \end{aligned} \quad (2.14)$$

$$G_{ab}(\tau) = -G_{ba}(-\tau), \quad G_{ab}(\tau)^* = -G_{ab}(-\tau), \quad G_{ab}(\tau + \beta) = -G_{ab}(\tau). \quad (2.15)$$

Note that when we set $\tilde{\mathcal{J}} = \mathcal{J}$ the effective action and the Schwinger-Dyson equation coincide with those in the Maldacena-Qi model [24] since the Hamiltonian reduces to that model. Also note that when we set $\tilde{\mathcal{J}} = 0$ the effective action and the Schwinger-Dyson equation coincide with those in the Kourkoulou-Maldacena model [36] if we identify $G_{LL}(\tau, \tau') = G_{RR}(\tau, \tau') = G_{\text{diag}}(\tau, \tau')$, $G_{LR}(\tau, \tau') = G_{\text{off}}(\tau, \tau')$.

By using the operator relations

$$\partial_\tau (e^{\tau H} \psi_i^a e^{-\tau H} \psi_i^a) |_{\tau \rightarrow +0} = [H, \psi_i^a] \psi_i^a = q H_{\text{SYK}}^{(a)} + \mu H_{\text{int}}, \quad (a = L, R) \quad (2.16)$$

together with the identification (2.12), we can express the energy $E = \frac{\langle \text{tr} H e^{-\beta H} \rangle_{J_{i_1 \dots i_q}^{(\alpha)}}}{\langle \text{tr} e^{-\beta H} \rangle_{J_{i_1 \dots i_q}^{(\alpha)}}}$ as

$$\frac{E}{N} = \left[\frac{1}{q} \partial_\tau G_{LL}(\tau, 0) + \frac{1}{q} \partial_\tau G_{RR}(\tau, 0) + i\mu \left(1 - \frac{2}{q} \right) G_{LR}(\tau, 0) \right]_{\tau \rightarrow +0}. \quad (2.17)$$

Using the Schwinger-Dyson equations (2.14) and the symmetry property of $G_{ab}(\tau)$ (2.15) it follows

$$\lim_{\tau \rightarrow +0} \partial_\tau G_{aa}(\tau, 0) = \sum_c \int d\tau \Sigma_{ac}(\tau) G_{ca}(-\tau) = - \sum_c \frac{s_{ac} \mathcal{J}_{ac}^2}{2q} \int d\tau (2G_{ac}(\tau))^q, \quad (2.18)$$

²These argument can be generalized to complex τ, τ' and we obtain $G_{ab}(u_1, u_2)^* = -G_{ab}(-u_1^*, -u_2^*)$, which we will use later in section 3.3.

hence the energy (2.17) can be further rewritten as

$$\frac{E}{N} = - \sum_{a,b} \frac{s_{ab} \mathcal{J}_{ab}^2}{2q^2} \int d\tau (2G_{ab}(\tau))^q + i\mu G_{LR}(0). \quad (2.19)$$

In the following sections, we study the solution of the Schwinger-Dyson equation both numerically and analytically.

3 Finite q , large N

In this section we study the two-coupled model (2.1) with $q = 4$ in the large N limit numerically by using the bilocal field formalism (2.7) with (2.8), (2.9).

3.1 Phase diagram

In the large N limit we can evaluate the partition function (2.8) by the solution of the equations of motion (2.9). If we define the Fourier transformation as

$$f(\tau) \rightarrow \hat{f}(\nu) = \int_0^\beta d\tau e^{i\nu\tau} f(\tau), \quad (3.1)$$

and also impose an ansatz $G_{RR}(\tau) = G_{LL}(\tau)$, the Euclidean Schwinger-Dyson equation (2.9) can be rewritten as

$$\begin{aligned} \hat{G}_{LL}(\nu) + \frac{i\nu + \hat{\Sigma}_{LL}(\nu)}{(i\nu + \hat{\Sigma}_{LL}(\nu))^2 + \hat{\Sigma}_{LR}(\nu)^2} &= 0, \\ \hat{G}_{LR}(\nu) - \frac{\hat{\Sigma}_{LR}(\nu)}{(i\nu + \hat{\Sigma}_{LL}(\nu))^2 + \hat{\Sigma}_{LR}(\nu)^2} &= 0, \\ \Sigma_{LL}(\tau) = \frac{\mathcal{J}^2}{q} (2G_{LL}(\tau))^{q-1}, \quad \Sigma_{LR}(\tau) = \frac{(-1)^{\frac{q}{2}} \tilde{\mathcal{J}}^2}{q} (2G_{LR}(\tau))^{q-1} + i\mu\delta(\tau), \end{aligned} \quad (3.2)$$

The partition function, or the free energy $F = -\frac{1}{\beta} \log Z$, can be evaluated in the large N limit by the solutions of (3.2) as

$$F \approx \min \left\{ \frac{1}{\beta} S_E[G_{ab}(\tau, \tau'), \Sigma_{ab}(\tau, \tau')] \mid (G_{ab}, \Sigma_{ab}): \text{solution of (3.2)} \right\}. \quad (3.3)$$

The set of equations (3.2) can be solved numerically for each values of $(q, \mathcal{J}, \tilde{\mathcal{J}}, \mu)$ and the inverse temperature $\beta = T^{-1}$. We performed the numerical analysis for $q = 4, \mathcal{J} = 1$ and various values $(\tilde{\mathcal{J}}, \mu, \beta)$. In particular, as we vary (μ, β) we obtained the following results:

- (i) When the temperature T is sufficiently large, there is a solution where $\frac{S_E}{\beta}$ is similar to the (annealed) free energy of two uncoupled SYK systems. We shall call this solution as two-black hole solution.
- (ii) As we decrease the temperature slowly (we have chosen $\Delta T = 0.0001$), this solution is deformed continuously until some temperature $T = T_{c,2BH}$. Once the temperature crosses $T_{c,2BH}$, the two-black hole solution ceases to exist and the numerical analysis detects another solution where the free energy is almost constant in T . We shall call this solution as wormhole solution.
- (iii) As we increase the temperature from $T < T_{c,2BH}$ the wormhole solution is deformed continuously until some temperature $T = T_{c,WH}$ which is greater than $T_{c,2BH}$. Once T exceeds $T_{c,WH}$ the wormhole solution disappears.
- (iv) When μ is larger than some critical value μ_* , (ii) and (iii) do not occur; the two-black hole solution and the wormhole solution merge to a single solution which exists at any value of the temperature.

See figure 2 and 3. These behaviors of the solution and the free energy are qualitatively the same as those for the case with $\tilde{\mathcal{J}} = \mathcal{J}$ [24, 30]. In the temperature regime $T_{c,2BH} < T < T_{c,WH}$ both the two-black hole solution and the wormhole solution exists, hence the free energy is given by the smaller one of the two values of S_E evaluated at these two solutions. We observe that the two values crosses at one point $T = T_c$, where the system undergoes a phase transition.

As we further vary $\frac{\tilde{\mathcal{J}}}{\mathcal{J}}$ we observed that these behaviors change in the following way:

- (v) $T_{c,WH}$ and T_c decrease as $\frac{\tilde{\mathcal{J}}}{\mathcal{J}}$ is decreased. On the other hand, $T_{c,2BH}$ also decreases, but it is almost independent of $\frac{\tilde{\mathcal{J}}}{\mathcal{J}}$ when μ is small. This is consistent with the fact that $T_{c,2BH}$ is determined as a property of the two-black hole solution where the off-diagonal component G_{LR}, Σ_{LR} are small and hence the correlation between $J_{i_1 i_2 \dots i_q}^{(L)}$ and $J_{i_1 i_2 \dots i_q}^{(R)}$ is less important. See figure 2.
- (vi) The critical value μ_* of μ where the phase transition disappears decreases as $\frac{\tilde{\mathcal{J}}}{\mathcal{J}}$ is decreased. See figure 4. From the results we also expect that μ_* becomes zero somewhere in the range $0.2 < \frac{\tilde{\mathcal{J}}^2}{\mathcal{J}^2} < 0.3$ (b and b'^2 in figure 4), that is, the phase transition completely disappears as $\frac{\tilde{\mathcal{J}}^2}{\mathcal{J}^2}$ is decreased below this value.

Though the observation that μ_c depends on $\frac{\tilde{\mathcal{J}}}{\mathcal{J}}$ might be surprising, it is consistent with the fact that for $\frac{\tilde{\mathcal{J}}}{\mathcal{J}} = 0$ our model (2.1) is equivalent in the large N limit to the single-side model [36] which does not exhibit phase transition at any value of μ [29].

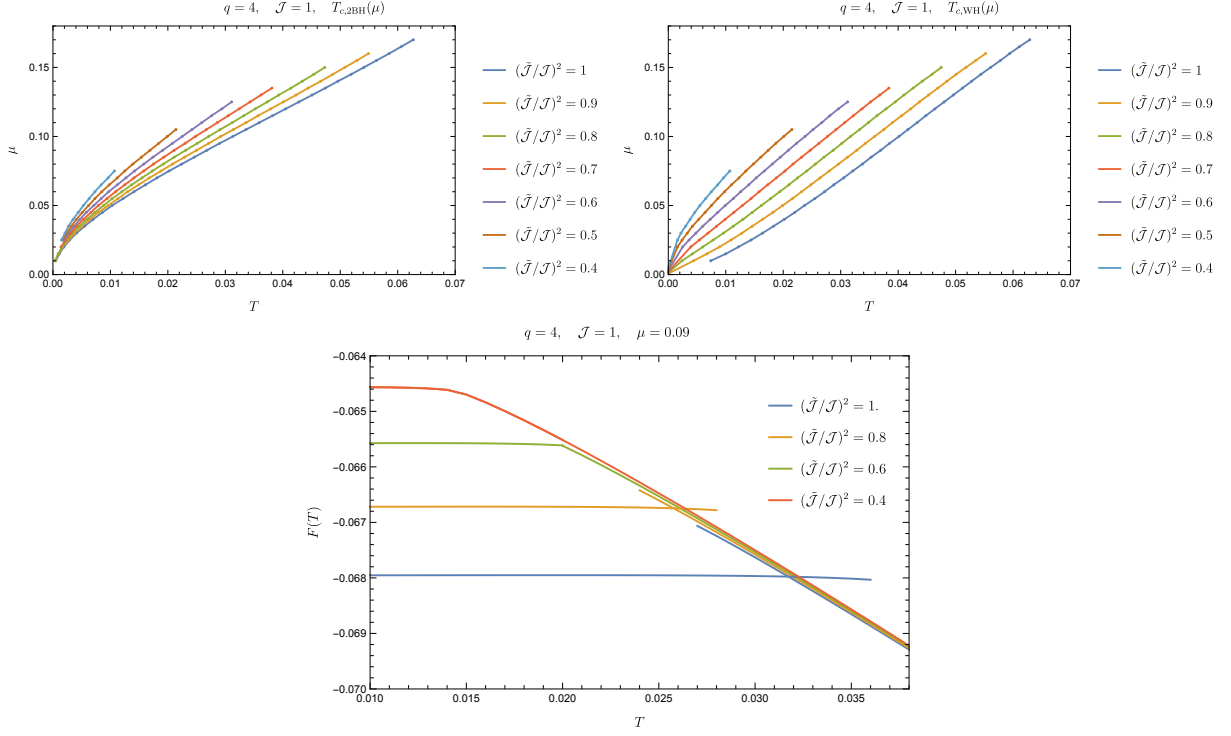


Figure 2: Top left/right: critical temperatures $T_{c,2BH}(\mu)$ and $T_{c,WH}(\mu)$ for various values of $\frac{\tilde{\mathcal{J}}}{\mathcal{J}}$. Bottom: free energy for the two solutions for $\mu = 0.09$ and various values of $\frac{\tilde{\mathcal{J}}}{\mathcal{J}}$ ($\frac{\tilde{\mathcal{J}}^2}{\mathcal{J}^2} = 0.4$ the two solutions are smoothly connected with each other).

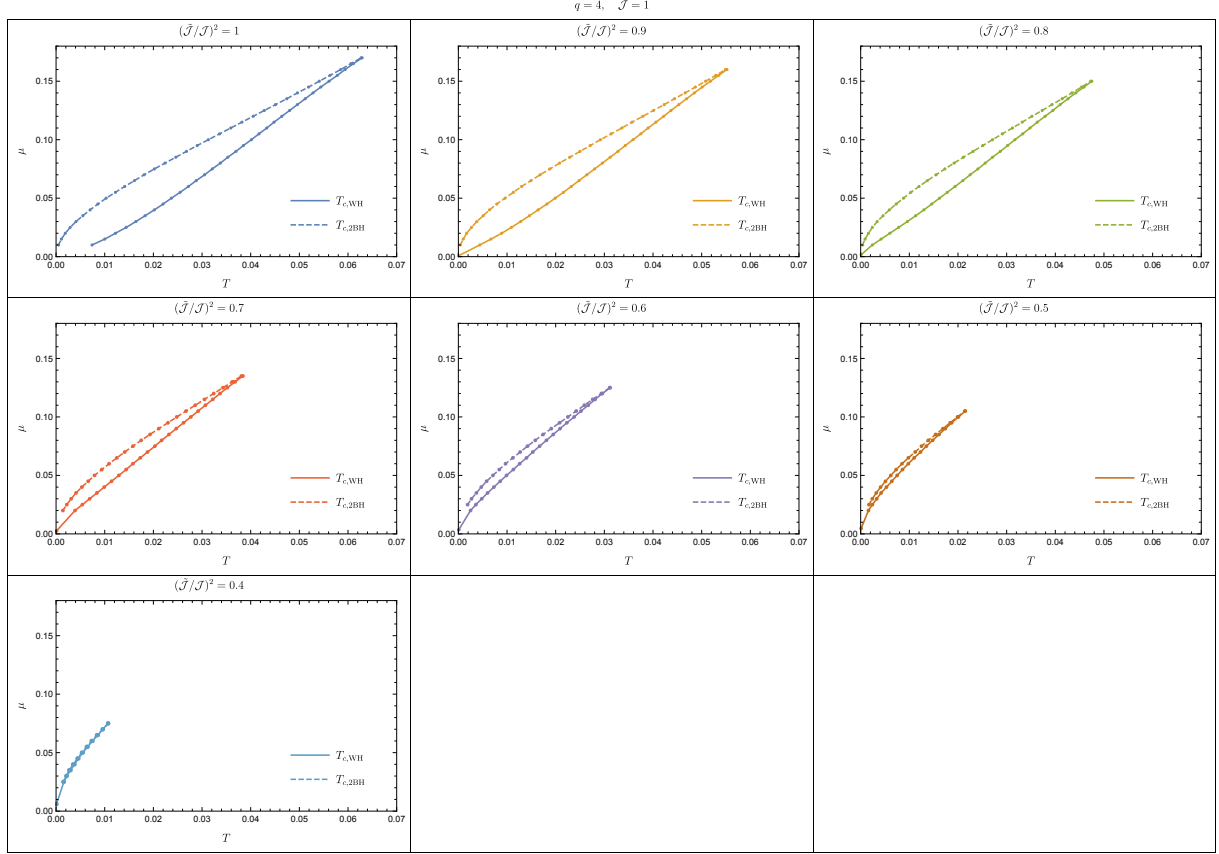


Figure 3: Phase diagram for various values of $\frac{\tilde{\mathcal{J}}}{\mathcal{J}}$. Points connected by the solid line are $T_{c,\text{WH}}(\mu)$ such that the wormhole solution does not exist for $T > T_{c,\text{WH}}$. Points connected by the dashed line are $T_{c,2\text{BH}}$ such that the two-black hole solution does not exist for $T < T_{c,2\text{BH}}$. The two lines intersect at a point (μ_*, T_*) ($T_* = T_{c,\text{WH}}(\mu_*) = T_{c,2\text{BH}}(\mu_*)$) which depends on $\frac{\tilde{\mathcal{J}}}{\mathcal{J}}$. In the regime where either $\mu > \mu_*$ or $T > T_*$ is satisfied, the wormhole solution and the two-black hole solution are smoothly connected with each other.

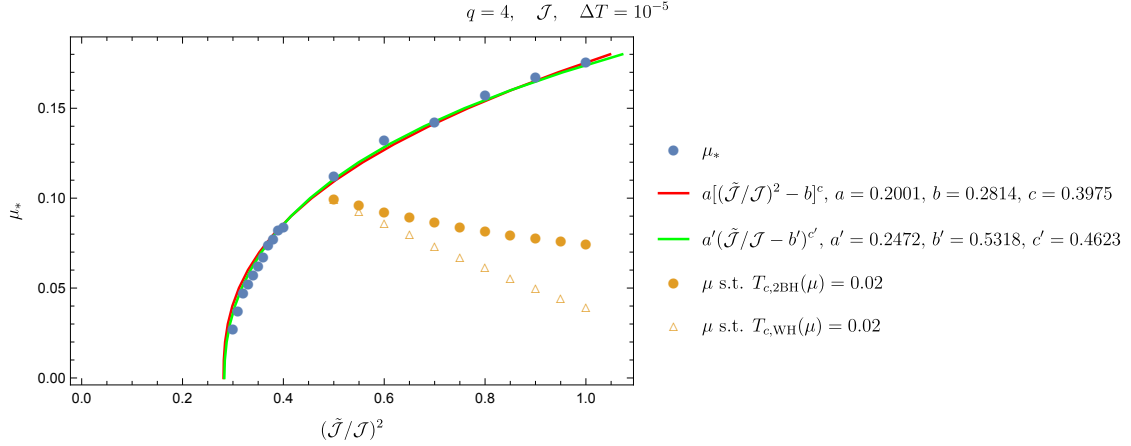


Figure 4: The critical value μ_* of μ for each $\frac{\tilde{\mathcal{J}}}{\mathcal{J}}$ such that the phase transition does not exist for $\mu > \mu_*$, with the red/green curve obtained by fitting with the ansatz $\mu_* = a((\frac{\tilde{\mathcal{J}}}{\mathcal{J}})^n - b)^c$. For comparison, we have also displayed the points on the phase transition lines in the $(\mu, \frac{\tilde{\mathcal{J}}^2}{\mathcal{J}^2})$ -plane with a fixed temperature $T = 0.02$, i.e., the points where $T_{c,2BH}(\mu; \frac{\tilde{\mathcal{J}}^2}{\mathcal{J}^2}) = 0.02$ and $T_{c,WH}(\mu; \frac{\tilde{\mathcal{J}}^2}{\mathcal{J}^2}) = 0.02$. Here we have determined α, c first by fitting the data of $\frac{d((\frac{\tilde{\mathcal{J}}}{\mathcal{J}})^n)}{d\mu_*}$ obtained by the numerical differentiation with the ansatz $\log \frac{d((\frac{\tilde{\mathcal{J}}}{\mathcal{J}})^n)}{d\mu_*} = (c - 1) \log \mu_* + \log(\alpha c)$ and then determined b by fitting again $(\frac{\tilde{\mathcal{J}}}{\mathcal{J}})^n$ with the ansatz $(\frac{\tilde{\mathcal{J}}}{\mathcal{J}})^n = (\frac{\mu_*}{a})^c + b$. We performed the fitting for $n = 1, 2$ and have found almost the same value of $b^{\frac{1}{n}}$, the value of $\frac{\tilde{\mathcal{J}}}{\mathcal{J}}$ where μ_* vanishes.

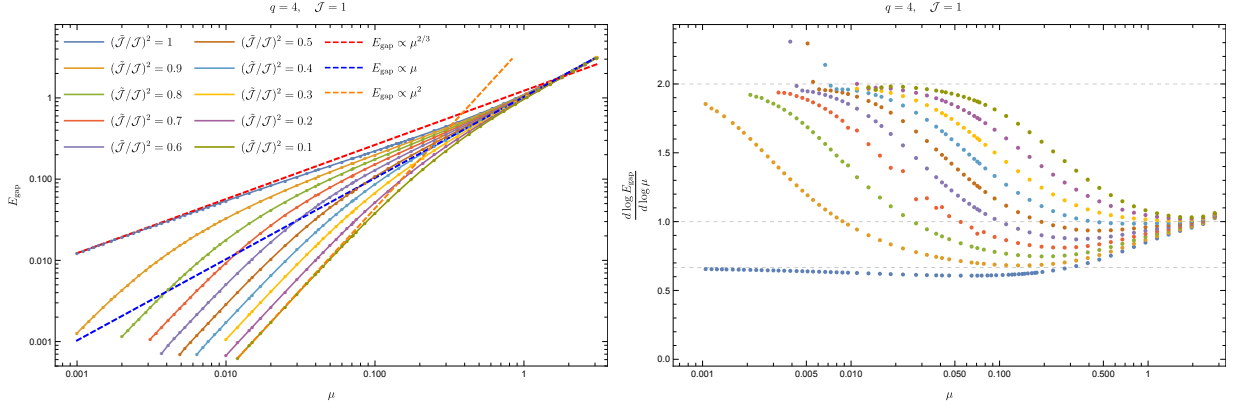


Figure 5: The energy gap E_{gap} for various values of $\tilde{\mathcal{J}}$ read off by fitting $G_{ab}(\tau)$ with the ansatz (3.4). Here the legends of the right plot are the same as those indicated in the left plot.

Notice that our claim (vi) for the absence of the phase transition is based on the observation that S_E obtained by decreasing T from high temperature regime and S_E obtained by increasing T from low temperature regime do not deviate at discrete points spaced with $\Delta T = 0.00001$, but this does not exclude the possibility that the phase transition exists with $T_{c,\text{WH}} - T_{c,2\text{BH}} < 0.00001$. In our approach it is in principle impossible to *prove* the absence of phase transition at $\mu > \mu_*$. As we see in section 4, however, we can rigorously show the absence of the phase transition in the large q limit.

3.2 Energy gap

Next we look at the energy gap E_{gap} of the two-coupled model (2.1) in the large N limit. In [29] we have observed that E_{gap} of the model (2.1) with $\tilde{\mathcal{J}} = \mathcal{J}$ [24] and E_{gap} of the single sided model [36] which is equivalent in the large N limit to the two coupled model with $\tilde{\mathcal{J}} = 0$ show different power law behavior for small μ : $E_{\text{gap}}(\tilde{\mathcal{J}} = \mathcal{J}) \sim \mu^{\frac{q}{2(q-1)}}$ and $E_{\text{gap}}(\tilde{\mathcal{J}} = 0) \sim \mu^{\frac{q}{q-2}}$. In this section we investigate how these two behaviors are interpolated as we vary $\tilde{\mathcal{J}}$ from 0 to 1.

The large N energy gap can be read off from the Euclidean two point functions $G_{ab}(\tau)$ in the low-temperature phase as [24]

$$G_{LL}(\tau) \sim \cosh\left[E_{\text{gap}}\left(\frac{\beta}{2} - \tau\right)\right], \quad G_{LR}(\tau) \sim \sinh\left[E_{\text{gap}}\left(\frac{\beta}{2} - \tau\right)\right]. \quad (1 \ll \tau \ll \beta) \quad (3.4)$$

By fitting $G_{ab}(\tau)$ with these ansatz we have obtained E_{gap} for $0.1 \leq \frac{\tilde{\mathcal{J}}^2}{\mathcal{J}^2} \leq 1$ as displayed in figure 5. We observe the followings

- For any value of μ , E_{gap} increase monotonically in $\frac{\tilde{\mathcal{J}}^2}{\mathcal{J}^2}$.
- When μ is sufficiently large, E_{gap} scales as $E_{\text{gap}} \sim \mu$ regardless of the value of $\frac{\tilde{\mathcal{J}}^2}{\mathcal{J}^2}$.
- When μ is sufficiently small, $E_{\text{gap}} \sim \mu^{2/3}$ for $\frac{\tilde{\mathcal{J}}^2}{\mathcal{J}^2} = 1$ while $E_{\text{gap}} \sim \mu^2$ for $\frac{\tilde{\mathcal{J}}^2}{\mathcal{J}^2} < 1$.
- When $\frac{\tilde{\mathcal{J}}^2}{\mathcal{J}^2}$ is less than 1 but close to 1, there is also an intermediate regime where $E_{\text{gap}} \sim \mu^{\frac{2}{3}}$. The range of the intermediate regime becomes wider in μ as $\frac{\tilde{\mathcal{J}}^2}{\mathcal{J}^2}$ approaches 1.

3.3 Real time response

Next we study real time dynamics of the two coupled model (2.3), in particular, the transmission amplitude T_{LR} [37] which measures how an excitation on the right site affects on the left site at late time, and the decay of the out-of-time-ordered four point function [38] which is characterized with the quantum chaos exponent λ_L . For this purpose we need to continue the $G\Sigma$ formalism for real τ (2.7)-(2.9) in section 2 to complex $u = \tau + it$, which can be done in the following way.³ First we define the two different components of the two point functions at $\text{Re}[u] = 0$, $G_{ab}^>, G_{ab}^<$, depending on how $\text{Re}[u]$ approaches 0:

$$\begin{aligned} G_{ab}^>(t_1, t_2) &= -iG_{ab}(it_1^-, it_2^+) = -i \lim_{\epsilon \rightarrow +0} G_{ab}(\epsilon + it_1, -\epsilon + it_2), \\ G_{ab}^<(t_1, t_2) &= -iG_{ab}(it_1^+, it_2^-) = -i \lim_{\epsilon \rightarrow +0} G_{ab}(-\epsilon + it_1, \epsilon + it_2), \end{aligned} \quad (3.5)$$

with which we also define the retarded/advanced components of the two point functions as

$$\begin{aligned} G_{ab}^R(t_1, t_2) &= \theta(t_1 - t_2)(G_{ab}^>(t_1, t_2) - G_{ab}^<(t_1, t_2)), \\ G_{ab}^A(t_1, t_2) &= \theta(t_2 - t_1)(G_{ab}^<(t_1, t_2) - G_{ab}^>(t_1, t_2)). \end{aligned} \quad (3.6)$$

We also define the $>, <, R, A$ components of $\Sigma_{ab}(u)$ at $u = it$ in the same ways.

With these notations the real time continuation of the Schwinger-Dyson equations (2.9) reduce to the followings

$$\begin{aligned} \tilde{G}_{LL}^R(\omega) &= \frac{-(-\omega + \tilde{\Sigma}_{RR}^R(\omega))}{(-\omega + \tilde{\Sigma}_{LL}^R(\omega))(-\omega + \tilde{\Sigma}_{RR}^R(\omega)) - (\tilde{\Sigma}_{LR}^R + i\mu)(\tilde{\Sigma}_{RL}^R - i\mu)}, \\ \tilde{G}_{LR}^R(\omega) &= \frac{\tilde{\Sigma}_{LR}^R(\omega) + i\mu}{(-\omega + \tilde{\Sigma}_{LL}^R(\omega))(-\omega + \tilde{\Sigma}_{RR}^R(\omega)) - (\tilde{\Sigma}_{LR}^R + i\mu)(\tilde{\Sigma}_{RL}^R - i\mu)}, \\ \tilde{G}_{RL}^R(\omega) &= \frac{\tilde{\Sigma}_{RL}^R(\omega) - i\mu}{(-\omega + \tilde{\Sigma}_{LL}^R(\omega))(-\omega + \tilde{\Sigma}_{RR}^R(\omega)) - (\tilde{\Sigma}_{LR}^R + i\mu)(\tilde{\Sigma}_{RL}^R - i\mu)}, \end{aligned}$$

³Note the calculations in this section are completely parallel to the case with $J_{i_1 \dots i_q}^{(L)} = J_{i_1 \dots i_q}^{(R)}$ in [30]. Hence we shall skip the details of the derivations which can be found in section 3 in [30].

$$\begin{aligned}\tilde{G}_{RR}^R(\omega) &= \frac{-(-\omega + \tilde{\Sigma}_{LL}^R(\omega))}{(-\omega + \tilde{\Sigma}_{LL}^R(\omega))(-\omega + \tilde{\Sigma}_{RR}^R(\omega)) - (\tilde{\Sigma}_{LR}^R + i\mu)(\tilde{\Sigma}_{RL}^R - i\mu)}, \\ \Sigma_{ab}^>(t_1, t_2) &= -\frac{i^q \mathcal{J}_{ab}^2}{q} s_{ab} G_{ab}^>(t_1, t_2)^{q-1},\end{aligned}\tag{3.7}$$

$$\begin{aligned}\Sigma_{ab}^R(t_1, t_2) &= \theta(t_1 - t_2)(\Sigma_{ab}^>(t_1, t_2) + \Sigma_{ba}^>(t_2, t_1)), \\ \tilde{G}_{ab}^>(\omega) &= \frac{\tilde{G}_{ab}^R(\omega) - (\tilde{G}_{ba}^R(\omega))^*}{1 + e^{-\beta\omega}},\end{aligned}\tag{3.8}$$

where we have defined the Fourier transform in real time t as

$$\tilde{f}^X(\omega) = \int_{-\infty}^{\infty} dt e^{i\omega t} f^X(t), \quad f^X(t) = \int_{-\infty}^{\infty} \frac{d\omega}{2\pi} e^{-i\omega t} \tilde{f}^X(\omega), \quad (f = G_{ab}, \Sigma_{ab}, \quad X = >, <, R, A).\tag{3.9}$$

Note that we can obtain $G_{ab}(u)$ for general $u \in \mathbb{C}$ from $\tilde{G}_{ab}^R(\omega)$ as

$$G_{ab}(u) = iG_{ab}^>(t = -iu) = i \int \frac{d\omega}{2\pi} e^{-\omega u} \frac{\tilde{G}_{ab}^R(\omega) - (\tilde{G}_{ba}^R(\omega))^*}{1 + e^{-\beta\omega}},\tag{3.10}$$

which we use to compute the chaos exponent in section 3.3.2.

3.3.1 Transmission amplitude in low temperature regime

Let us define the transmission amplitude $T_{LR}(t)$ as $T_{LR}(t) = 2|G_{LR}^>(t)|$, which measures the probability to find the excitation of ψ_i^L at time t after the insertion of ψ_i^R at time $t = 0$ [37]. We have displayed $T_{LR}(t)$ for $q = 4, \mathcal{J} = 1, \mu = 0.1, T = 0.019$ and various values of $\frac{\tilde{\mathcal{J}}^2}{\mathcal{J}^2}$ in figure 6. We find that the transmission is reduced by decreasing LR correlation $\frac{\tilde{\mathcal{J}}^2}{\mathcal{J}^2}$. Note that when the temperature is sufficiently small, $G_{LR}^>(t)$ is well approximated by a single quasi-particle with the speed ω_1 and a finite life time Γ_1 : $G_{LR}^>(t) \sim e^{-i\omega_1 t - \Gamma_1 t}$. Hence the suppression of $T_{LR}(t)$ can be explained by the decrease of ω_1 and increase of Γ_1 , both of which are encoded in the first peak of the spectral function $\rho_{LR}(\omega) = -2\text{Re}[\tilde{G}_{LR}(\omega)]$, as $\frac{\tilde{\mathcal{J}}^2}{\mathcal{J}^2}$ is decreased. See figure 7.

3.3.2 Chaos exponent

To compute the chaos exponent, we consider the four point function

$$\frac{1}{N^2} \sum_{i,j}^N \langle \psi_i^a(u_1) \psi_i^b(u_2) \psi_j^c(u_3) \psi_j^d(u_4) \rangle = \frac{1}{Z} \int \mathcal{D}G_{ab} \mathcal{D}\Sigma_{ab} G_{ab}(u_1, u_2) G_{cd}(u_1, u_2) e^{-NS}.\tag{3.11}$$

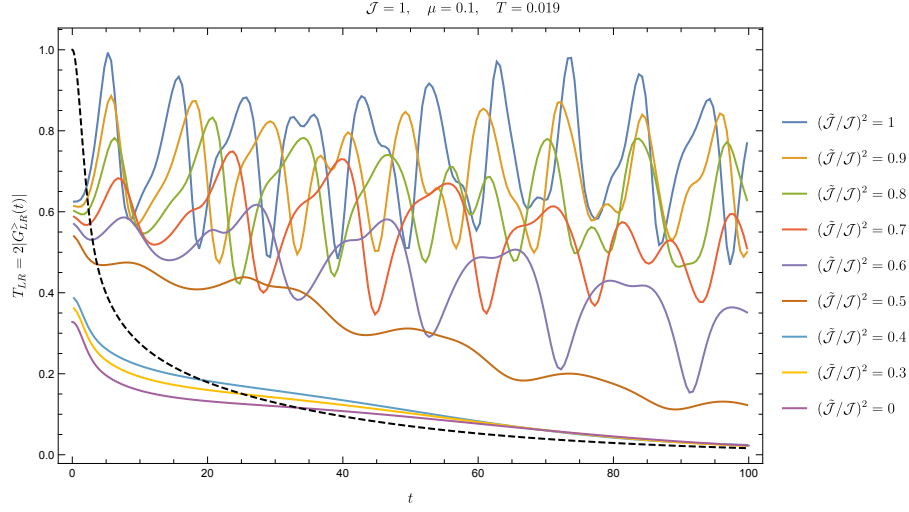


Figure 6: Transmission amplitude $T_{LR}(t) = 2|G_{LR}^>(t)|$ for various values of $\frac{\tilde{\mathcal{J}}^2}{\mathcal{J}^2}$ in the low-temperature phase. Note that for $\frac{\tilde{\mathcal{J}}^2}{\mathcal{J}^2} = 0.4$ there are no phase transition for $\mu = 0.1$ (see figure 3), hence $(\mu, T) = (0.1, 0.019)$ belongs to the supercritical regime. For comparison we have also plotted $2|G^>(t)|$ for a single SYK model (dashed black line).

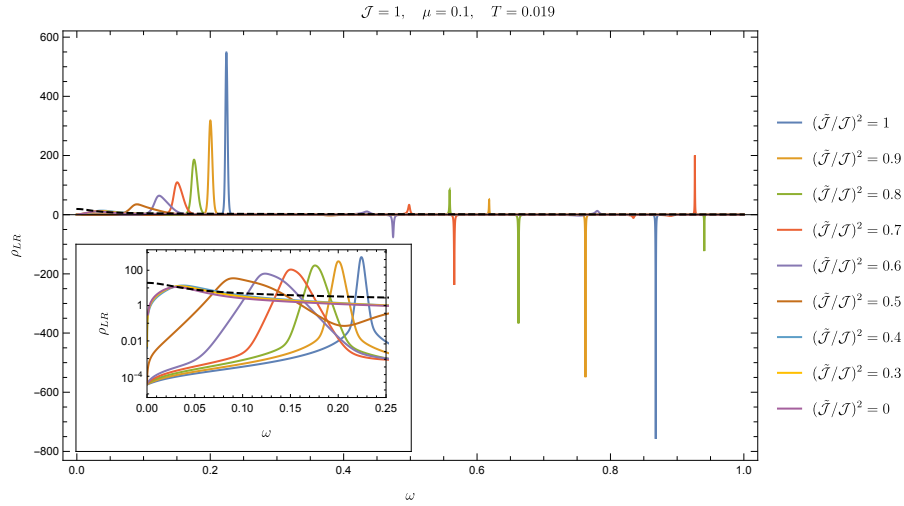


Figure 7: Spectral function $\rho_{LR}(\omega) = -2\text{Re}[\tilde{G}_{LR}^R(\omega)]$.

with $u_1 = \frac{3\beta}{4} + it_1$, $u_2 = \frac{\beta}{4} + it_2$, $u_3 = \frac{\beta}{2}$, $u_4 = 0$. The chaos exponent λ_L is given by the following late-time behavior of the four point function:

$$\frac{1}{N^2} \sum_{i,j}^N \langle \psi_i^a(u_1) \psi_i^b(u_2) \psi_j^c(u_3) \psi_j^d(u_4) \rangle = G_{ab}(u_1, u_2) G_{cd}(u_3, u_4) + \frac{1}{N} \mathcal{F}_{abcd}(u_1, u_2, u_3, u_4),$$

$$\mathcal{F}_{abcd}(u_1, u_2, u_3, u_4) \sim e^{\frac{\lambda_L(t_1+t_2)}{2}} \quad (t_1, t_2 \gg 1). \quad (3.12)$$

In the large N limit and at late time we find that $\mathcal{F}_{abcd}(t_1, t_2)$ obeys the following equation [30]

$$\mathcal{F}_{abcd}(t_1, t_2) \approx \sum_{ef} \int dt dt' \mathcal{K}_{abef}^R(t_1, t_2, t, t') \mathcal{F}_{efcd}(t, t'),$$

$$\mathcal{K}_{abcd}^R(t_1, t_2, t_3, t_4) = -\frac{\mathcal{J}_{cd}^2 2^{q-1} (q-1)}{q} G_{ac}^R(t_1 - t_3) G_{bd}^R(t_2 - t_4) s_{cd} G_{cd} \left(\frac{\beta}{2} + i(t_3 - t_4) \right)^{q-2}. \quad (3.13)$$

If we substitute the ansatz $\mathcal{F}_{abcd}(t_1, t_2) = e^{\frac{\lambda_L(t_1+t_2)}{2}} f_{abcd}(t_{12})$ this equation can be rewritten as an eigenequation of $f_{ab..}(t)$ with eigenvalue 1 [30]:

$$\sum_{e,f} \int dt' \mathcal{M}_{abef}(\lambda_L; t, t') f_{efcd}(t') \approx f_{abcd}(t)$$

$$\mathcal{M}_{abcd}(\lambda_L; t, t') = -\frac{\mathcal{J}_{cd}^2 2^{q-1} (q-1)}{q} e^{-\frac{\lambda_L(t-t')}{2}} \left[\int dt'' G_{ac}^R(t - t' - t'') G_{bd}^R(-t'') e^{\lambda_L t''} \right] s_{cd} G_{cd} \left(\frac{\beta}{2} + it' \right)^{q-2}. \quad (3.14)$$

The quantum chaos exponent λ_L can be determined so that the largest eigenvalue of the λ_L -dependent kernel $\mathcal{M}_{abcd}(\lambda_L; t, t')$ crosses 1.

Notice that (3.14) can be decomposed into the following two equations with $\sigma = \pm 1$ [30]

$$\begin{pmatrix} f_{2,LL}(t) + \sigma f_{2,RR}(t) \\ f_{2,LR}(t) - \sigma f_{2,RL}(t) \end{pmatrix}_a = \sum_b \int dt' \mathcal{M}_{ab}(\sigma, \lambda_L; t, t') \begin{pmatrix} f_{2,LL}(t') + \sigma f_{2,RR}(t') \\ f_{2,LR}(t') - \sigma f_{2,RL}(t') \end{pmatrix}_b, \quad (3.15)$$

where $a, b = 1, 2$ and

$$\mathcal{M}_{ab}(\sigma, \lambda_L; t, t') = \begin{pmatrix} (M_{1,LLLL}(t-t') + \sigma M_{1,LRLR}(t-t')) M_{2,LL}(t') & (M_{1,LLLR}(t-t') - \sigma M_{1,LRLR}(t-t')) M_{2,LL}(t') \\ -(M_{1,LLLR}(t-t') - \sigma M_{1,LRLR}(t-t')) M_{2,LR}(t') & (M_{1,LLLL}(t-t') + \sigma M_{1,LRLR}(t-t')) M_{2,LR}(t') \end{pmatrix} \quad (3.16)$$

with

$$f_{2,ab}(t_{12}) = e^{\frac{\lambda_L t_{12}}{2}} f_{ab}(t_{12}),$$

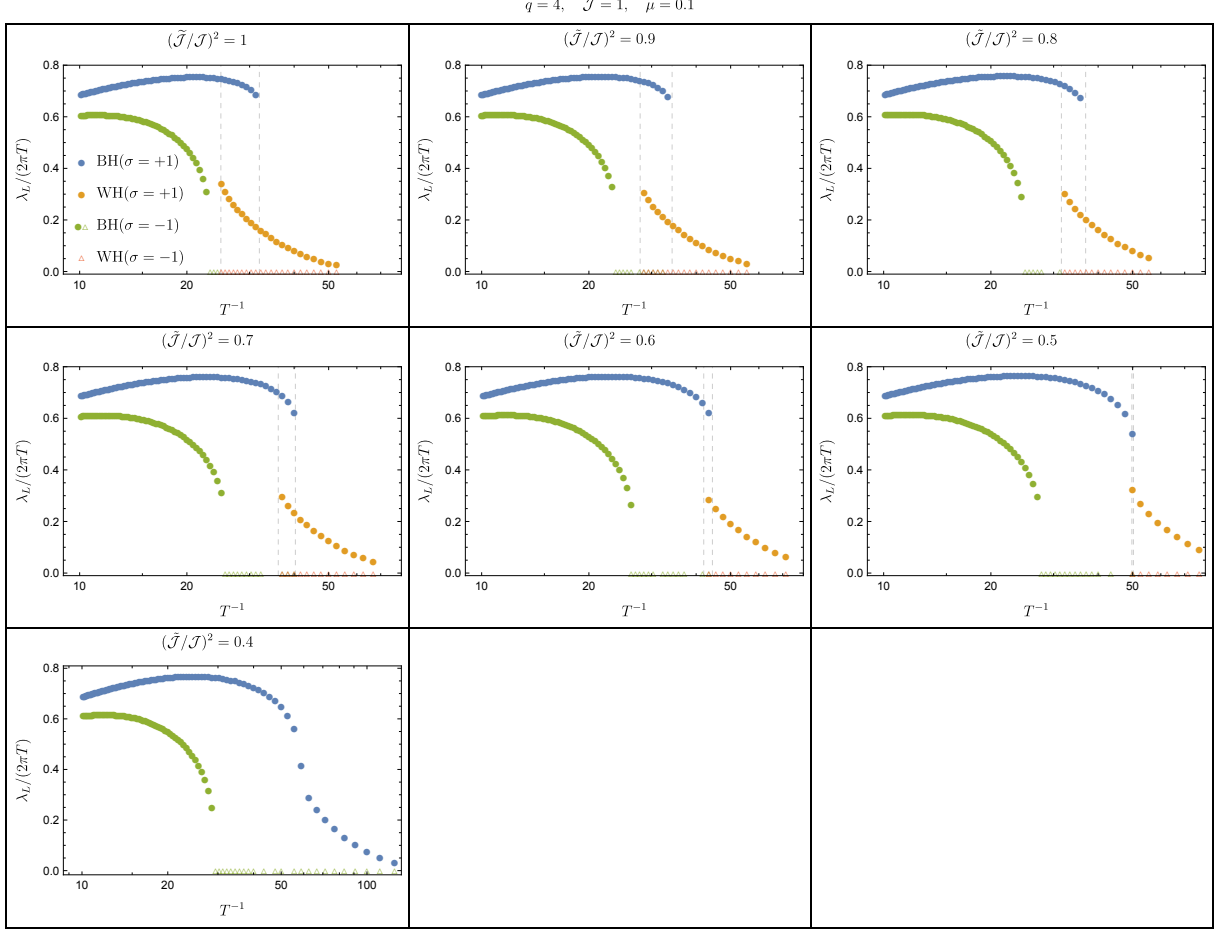


Figure 8: The chaos exponent λ_L for the two sectors $\sigma = \pm 1$. Here we have displayed the data points where the largest absolute value of the eigenvalues of $\mathcal{M}_{ab}(-1, \lambda_L; t, t')$ does not cross 1 in $0 < \lambda_L \leq 2\pi T$ with empty triangle markers.

$$\begin{aligned}
 M_{1,abcd}(t) &= \int dt' G_{ab}^R(t-t') G_{cd}^R(-t') e^{\lambda_L t'}, \\
 M_{2,ab}(t) &= -\frac{\mathcal{J}_{ab}^2 2^{q-1} (q-1)}{q} s_{ab} G_{ab} \left(\frac{\beta}{2} + it \right)^{q-2}.
 \end{aligned} \tag{3.17}$$

Hence we can compute the chaos exponent $\lambda_L(\sigma)$ for each sector rather than the chaos exponent of the full system $\lambda_L = \max\{\lambda_L(1), \lambda_L(-1)\}$.

By performing a binary search for the value of λ_L in the range $0 < \lambda_L \leq 2\pi T$ such that the largest eigenvalue of $\mathcal{M}_{ab}(\sigma, \lambda_L; t, t')$ is 1, we obtained the chaos exponent for $\sigma = \pm 1$ and various values of $\tilde{\mathcal{J}}^2/\mathcal{J}^2$, as displayed in figure 8. We found that as $\tilde{\mathcal{J}}^2/\mathcal{J}^2$ is decreased the chaos exponent of each sector increases while their temperature dependence remains qualitatively the same. This result may be interpreted in the following way. Let us assume that the chaos

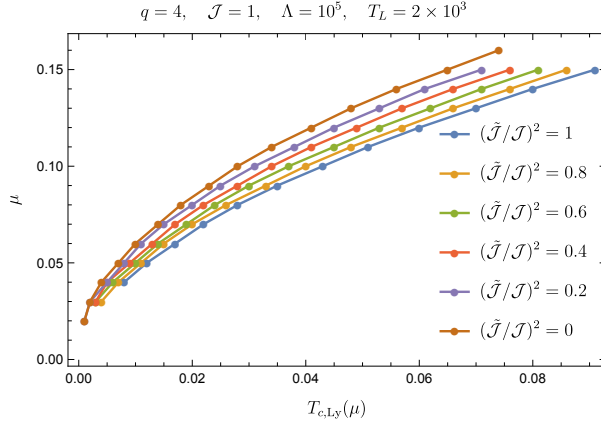


Figure 9: The temperature $T_{c,Ly}$ where the binary search to determine $\lambda_L(-1)$ fails.

exponent is associated with the operator growth over a single side (say Left). In the two-coupled system the operator growth in a single side should be reduced due to the leakage of the operator to the operators supported on the other side. As we have seen in the previous section, as $\frac{\tilde{\mathcal{J}}^2}{\mathcal{J}^2}$ is decreased the LR transmission becomes suppressed. Hence the chaos exponent is expected to become larger as $\frac{\tilde{\mathcal{J}}^2}{\mathcal{J}^2}$ is decreased, which is consistent with the results in figure 8.

Interestingly we also found that when the temperature is lower than some critical value $T_{c,Ly}(\frac{\tilde{\mathcal{J}}}{\mathcal{J}}, \mu)$ (which is larger than $T_{c,2BH}$), the absolute values of the eigenvalues of $\mathcal{M}_{ab}(-1, \lambda_L; t, t')$ are smaller than 1 for any value of λ_L in $0 < \lambda_L \leq 2\pi T$. This would imply that there are no exponentially growing modes in $\sigma = -1$ sector for $T < T_{c,Ly}$. In figure 9 we display the observed values of $T_{c,Ly}$ for various $\tilde{\mathcal{J}}/\mathcal{J}$ and μ .

4 large q limit

In the large q limit, we can study the $J_{i_1 \dots i_q}^{(L)} \neq J_{i_1 \dots i_q}^{(R)}$ model analytically. In this section we study this limit and compare with the former section of the numerical analysis at finite q .

4.1 large q limit at zero temperature

In the large q limit, the $G\Sigma$ action reduces to the Liouville action:

$$\begin{aligned} \frac{S_E}{N} = & \frac{1}{8q^2} \int d\tau_1 \int d\tau_2 \left(\partial_{\tau_1} g_{LL}(\tau_1, \tau_2) \partial_{\tau_2} g_{LL}(\tau_1, \tau_2) - \partial_{\tau_1} g_{LR}(\tau_1, \tau_2) \partial_{\tau_2} g_{LR}(\tau_1, \tau_2) \right) \\ & - \frac{\mathcal{J}^2}{2q^2} \int d\tau_1 \int d\tau_2 e^{g_{LL}(\tau_1, \tau_2)} - \frac{\tilde{\mathcal{J}}^2}{2q^2} \int d\tau_1 \int d\tau_2 e^{g_{LR}(\tau_1, \tau_2)} - \frac{\hat{\mu}}{2q^2} \int d\tau g_{LR}(\tau, \tau), \end{aligned} \quad (4.1)$$

with the following ansatz for the large q expansion

$$\begin{aligned} G_{LL}(\tau) &= G_{RR}(\tau) = \frac{1}{2} \text{sgn}(\tau) \left(1 + \frac{1}{q} g_{LL}(\tau) + \dots \right), \\ G_{LR}(\tau) &= -G_{RL}(\tau) = \frac{i}{2} \left(1 + \frac{1}{q} g_{LR}(\tau) + \dots \right), \end{aligned} \quad (4.2)$$

and we also scale μ so that $\hat{\mu} = \mu q$ is kept finite in the large q limit. At small temperature and the late time of order $\tau \sim q$, this approximation is not valid because of the exponential decay of the correlation functions. In this case, we also consider the solution in $\tau \gg q$ regime and impose the matching condition between $\tau \ll q$ and $\tau \gg q$ solutions, as we discuss in section 4.2. The Schwinger-Dyson equation reduces to the following two equation:

$$\begin{aligned} \partial_\tau^2 g_{LL}(\tau) &= 2\mathcal{J}^2 e^{g_{LL}(\tau)}, \quad (\text{for } \tau > 0) \\ \partial_\tau^2 g_{LR}(\tau) &= -2\tilde{\mathcal{J}}^2 e^{g_{LR}(\tau)} - 2\hat{\mu}\delta(\tau), \end{aligned} \quad (4.3)$$

with the boundary conditions

$$\begin{aligned} g_{LL}(0) &= 0, \quad \partial_\tau g_{LR}(0^+) = -\hat{\mu}, \\ g_{LL}(\tau) - g_{LR}(\tau) &\rightarrow 0, \quad \text{as } \tau \rightarrow \infty. \end{aligned} \quad (4.4)$$

The general solutions of the equations (4.3) are

$$\begin{aligned} e^{g_{LL}(\tau)} &= \frac{\alpha^2}{\mathcal{J}^2 \sinh^2(\alpha|\tau| + \gamma)}, \\ e^{g_{LR}(\tau)} &= \frac{\tilde{\alpha}^2}{\tilde{\mathcal{J}}^2 \cosh^2(\tilde{\alpha}|\tau| + \tilde{\gamma})}, \end{aligned} \quad (4.5)$$

with constants of the integration $\alpha, \tilde{\alpha}, \gamma, \tilde{\gamma}$. These parameters are determined by the boundary conditions which depend on the temperature.

Each of the boundary conditions (4.4) fixes the constants of integration in a following way. First, the boundary conditions at $\tau = 0$ give the relations

$$\begin{aligned} g_{LL}(0) = 0 &\quad \Rightarrow \quad \frac{\alpha}{\mathcal{J} \sinh \gamma} = 1 \\ \partial_\tau g_{LR}(0^+) = -\hat{\mu} &\quad \Rightarrow \quad 2\tilde{\alpha} \tanh \tilde{\gamma} = \hat{\mu}, \end{aligned} \quad (4.6)$$

whereas the boundary condition at $\tau = \infty$ gives

$$g_{LL}(\tau) - g_{LR}(\tau) \rightarrow 0, \quad \text{as } \tau \rightarrow \infty \quad \Rightarrow \quad \tilde{\gamma} = \gamma + s, \quad \alpha = \tilde{\alpha}. \quad (4.7)$$

Here $s = \log \frac{\tilde{\mathcal{J}}}{\mathcal{J}}$ is a positive parameter and vanish when $\tilde{\mathcal{J}} = \mathcal{J}$. Finally, γ satisfies the equation

$$\sinh \gamma \tanh(\gamma + s) = \frac{\hat{\mu}}{2\mathcal{J}}, \quad (4.8)$$

and other parameters are determined through γ . The physical gap E_{gap} is given by

$$E_{gap} = \frac{2\alpha}{q}. \quad (4.9)$$

For small $j \equiv \mathcal{J} - \tilde{\mathcal{J}}$ limit, we can separate the scale of Maldacena-Qi behavior and Kourkoulou-Maldacena behavior. When $j \ll \mu$, we can ignore the parameter s and we obtain

$$\sinh \gamma \tanh \gamma = \frac{\hat{\mu}}{2\mathcal{J}}, \quad (4.10)$$

which is exactly the same equation with the Maldacena-Qi model. γ is given by

$$\tanh^2 \gamma = \frac{\epsilon}{2}(\sqrt{4 + \epsilon^2} - \epsilon), \quad \epsilon = \frac{\hat{\mu}}{2\mathcal{J}}. \quad (4.11)$$

In the range $j \ll \hat{\mu} \ll \mathcal{J}$, we can expand as

$$\gamma \approx \sqrt{\epsilon} = \sqrt{\frac{\hat{\mu}}{2\mathcal{J}}}, \quad \alpha = \mathcal{J} \sinh \gamma \approx \sqrt{\frac{\hat{\mu}\mathcal{J}}{2}} \quad (4.12)$$

and the gap is given by

$$E_{gap} = \frac{2\alpha}{q} \approx \frac{\sqrt{2\hat{\mu}\mathcal{J}}}{q}. \quad (4.13)$$

This parameter regime exists only when $j \ll \mathcal{J}$. In the regime $\hat{\mu} \ll j$, we can ignore the γ from the term $\tanh(\gamma + s)$. Therefore we obtain the equation

$$\sinh \gamma \tanh s \approx \frac{\hat{\mu}}{2\mathcal{J}}. \quad (4.14)$$

We can evaluate $\tanh s$ as

$$\tanh s = \frac{e^s - e^{-s}}{e^s + e^{-s}} = \frac{\mathcal{J}^2 - \tilde{\mathcal{J}}^2}{\mathcal{J}^2 + \tilde{\mathcal{J}}^2} \quad (4.15)$$

Then, γ is evaluated as

$$\sinh \gamma \approx \frac{\hat{\mu}}{2\mathcal{J} \tanh s}. \quad (4.16)$$

When $\tilde{\mathcal{J}} = 0$ this reduces to the relation of Kourkoulou-Maldacena model. This parameter regime always exists but we need to take $\hat{\mu}$ to be smaller than j . When $\tilde{\mathcal{J}} = \mathcal{J}$, i.e., the perfect correlation between left and right SYK model, this regime vanishes which occurs in the Maldacena-Qi model. The parameter α becomes $\alpha \approx \frac{\hat{\mu}}{2 \tanh s}$. The mass gap in this limit becomes

$$E_{gap} = \frac{2\alpha}{q} \approx \frac{\hat{\mu}}{q \tanh s}. \quad (4.17)$$

For $j = \mathcal{J}$, i.e., when there are no correlations between $J_{i_1 \dots i_q}^{(L)}$ and $J_{i_1 \dots i_q}^{(R)}$, we have $E_{gap} = \frac{\hat{\mu}}{q}$, which is the same with that of the Kourkoulou-Maldacena model.

Let us study how the behavior of E_{gap} in μ changes when we decrease μ . The plot of E as a function of μ is shown in figure 10. The power of the gap in μ is defined as $\frac{d \log E_{gap}}{d \log \mu}$. Here we take the derivative with respect to μ while we fix \mathcal{J} and $\tilde{\mathcal{J}}$. Then s is also fixed and this is equivalent to take the derivative with respect to γ while fixing s . This becomes

$$\frac{d \log E_{gap}}{d \log \mu} = \frac{\hat{\mu}}{\alpha} \frac{\partial \gamma}{\partial \hat{\mu}} \frac{\partial \alpha}{\partial \gamma} = \frac{\sinh(\gamma + s) \cosh(\gamma + s)}{\sinh(\gamma + s) \cosh(\gamma + s) + \tanh \gamma}. \quad (4.18)$$

The plot of (4.18) is shown in figure 11. We can see that for very small j , there is a region where the power in μ is almost 1/2, which is the behavior in the Maldacena-Qi model. On the other hand, even for small j , the power in μ approaches to 1 for sufficiently small μ as we expect.

The real time correlation function is obtained by analytically continuing to the Lorentzian time. At low temperature of order $\beta = O(q \log q)$ we see that there are no decay and the return amplitude just oscillate. This is because the decay rate is of order $e^{-(\frac{q}{2}-1)E_{gap}}$, which is non-perturbatively small in q [30, 39] at large q limit, and we did not take into account this decay rate at large q . Since the decay rate is also suppressed by the energy gap E_{gap} , the decay rate will increase as we decrease the correlation of the random couplings between the two sides.

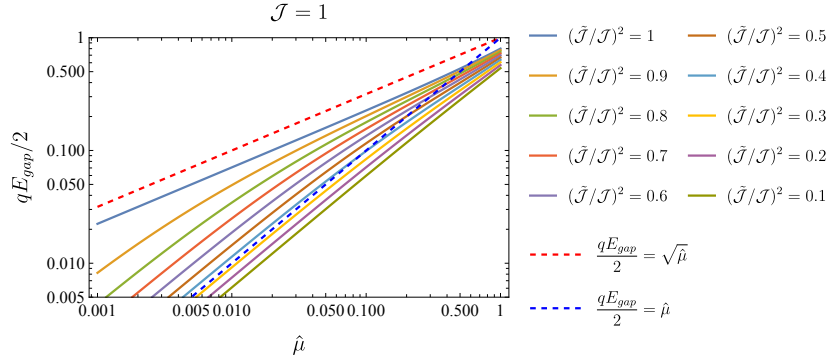


Figure 10: Plot of E_{gap} as a function of $\hat{\mu}$.

4.2 Finite temperature

For $\tau \ll q$ we can still use the solution (4.5) together with the boundary conditions at $\tau \rightarrow 0$ (4.6). For $\tau \gg q$, we can make a different approximation for the Schwinger-Dyson equation (2.14) which goes as follows. First, from the second equation in (2.9) we can approximate the self energy $\Sigma_{ab}(\tau)$ at the time scale of $G_{ab}(\tau)$ by the delta function configurations (see section

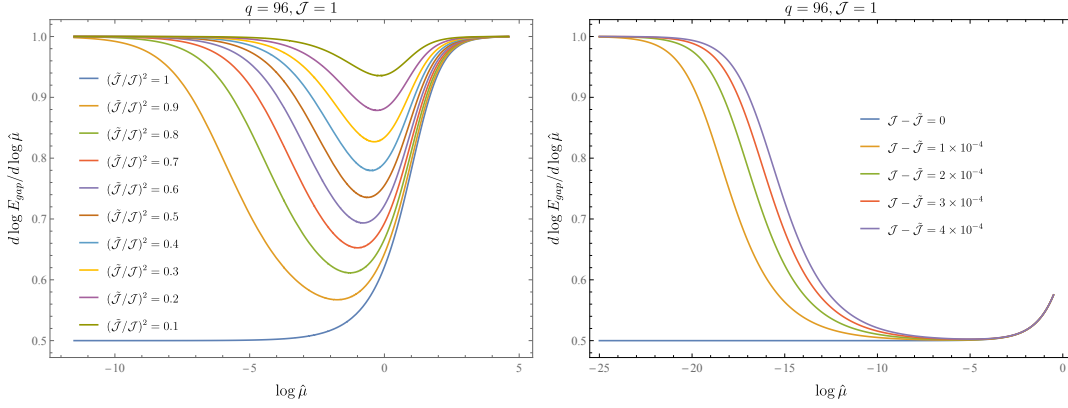


Figure 11: Plots of the power of E_{gap} in $\hat{\mu}$.

5.4 in [24])

$$\Sigma_{LL}(\tau), \Sigma_{RR}(\tau) \approx \rho \partial_\tau \delta(\tau), \quad \Sigma_{LR}(\tau) = -\Sigma_{RL}(\tau) \approx -i\nu \delta(\tau), \quad \nu = i \int_0^\beta \Sigma_{LR}(\tau) d\tau = \frac{2\tilde{\alpha}}{q}, \quad (4.19)$$

where ρ is a constant of order $\mathcal{O}(q^{-1})$. We have evaluated the last integration by using $G_{LR}(\tau)$ in the small τ regime (4.2),(4.5) which gives $i\Sigma_{LR}(\tau) \approx \frac{\tilde{\alpha}^2}{q \cosh^2(\tilde{\alpha}|\tau| + \tilde{\gamma})} + \mu\delta(\tau)$, and replacing the domain of integration with $(-\infty, \infty)$. With (4.19), the other Schwinger-Dyson equation is simplified as

$$(1 - \rho)\partial_\tau G_{LL}(\tau) - i\nu G_{LR}(\tau) = 0, \quad (4.20)$$

$$(1 - \rho)\partial_\tau G_{LR}(\tau) + i\nu G_{LL}(\tau) = 0, \quad (4.21)$$

We can ignore ρ in each equation since it gives a sub-leading correction in the large q limit. Solving these equations we have

$$G_{LL}(\tau) = A \cosh \left[\nu \left(\frac{\beta}{2} - \tau \right) \right], \quad G_{LR}(\tau) = iA \sinh \left[\nu \left(\frac{\beta}{2} - \tau \right) \right], \quad (4.22)$$

where A is an integration constant. The other integration constant (translation in τ) is fixed by the conditions $G_{LL}(\tau) = G_{LL}(\beta - \tau)$, $G_{LR}(\tau) = -G_{LR}(\beta - \tau)$ which follows from (2.15).

Let us define $\sigma = qe^{-\beta\nu}$ as a new parameter corresponding to the temperature, and assume that σ is of order $\mathcal{O}(q^0)$ (i.e., $\beta = \mathcal{O}(q \log q)$). Matching the two solutions in the overlapping regime, i.e., the large τ expansion of the solution for $\tau \ll q$ with the small τ expansion of the solution for $\tau \gg q$ as

$$G_{LL}(\tau) \approx \frac{1}{2} + \frac{1}{q} \log \frac{2\alpha}{\mathcal{J}} - \frac{\gamma}{q} - \frac{\alpha\tau}{q} \approx A \left(\cosh \frac{\nu\beta}{2} - \nu\tau \sinh \frac{\nu\beta}{2} \right),$$

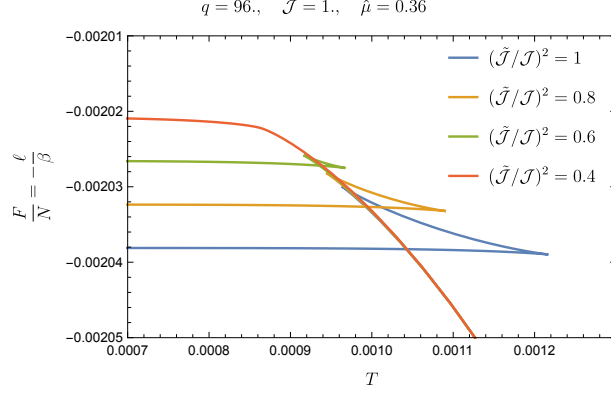


Figure 12: Plots of the free energy as a function of the temperature for representative $\tilde{\mathcal{J}}/\mathcal{J}$.

$$-iG_{LR}(\tau) \approx \frac{1}{2} + \frac{1}{q} \log \frac{2\tilde{\alpha}}{\tilde{\mathcal{J}}} - \frac{\tilde{\gamma}}{q} - \frac{\tilde{\alpha}\tau}{q} \approx A \left(\sinh \frac{\nu\beta}{2} - \nu\tau \cosh \frac{\nu\beta}{2} \right), \quad (4.23)$$

we can find the integration constants as

$$\tilde{\alpha} = \alpha, \quad \tilde{\gamma} = \gamma + s + \sigma, \quad \alpha = \mathcal{J} \sinh \gamma, \quad \hat{\mu} = 2\tilde{\alpha} \tanh \tilde{\gamma}. \quad (4.24)$$

Using the relation between the correlation functions and the energy (2.17) we obtain

$$\begin{aligned} \frac{E}{N} &= \frac{1}{2q} \partial_\tau g_{LL}(0) + \frac{1}{2q} \partial_\tau g_{RR}(0) + i\mu \left(1 - \frac{2}{q}\right) \frac{i}{2} \left(1 + \frac{1}{q} g_{LR}(0)\right) \\ &= -\frac{2\mathcal{J}}{q^2} \cosh \gamma - \frac{\hat{\mu}}{2q} + \frac{\hat{\mu}}{q^2} \left(1 + \log \frac{e^s \sinh \gamma}{\cosh \tilde{\gamma}}\right). \end{aligned} \quad (4.25)$$

The effective action $\ell = \frac{1}{N} \log Z$ is then (see appendix A)

$$\ell(\sigma, \gamma) = \frac{\tanh \tilde{\gamma} \log \frac{q}{\sigma}}{q} \left(\frac{q}{2} - 1 + \frac{1}{\tanh \gamma \tanh \tilde{\gamma}} + \log \frac{\sinh \gamma}{\cosh \tilde{\gamma}} + \frac{\sigma}{\tanh \tilde{\gamma}} + s \right) + \frac{\sigma}{q}. \quad (4.26)$$

Now we study the free energy $\frac{F}{N} = -\frac{\ell}{\beta}$ for representative $\tilde{\mathcal{J}}$. This can be worked out in the following way. First we choose $q, \mathcal{J}, \tilde{\mathcal{J}}, \hat{\mu}$ to a particular set of values. Then, by using the relations $\hat{\mu} = 2\mathcal{J} \sinh \gamma \tanh \tilde{\gamma}$ (4.24) and $\beta = -\frac{1}{2\mathcal{J} \sinh \gamma} \log \frac{\sigma}{q}$ we can compute $\gamma(\sigma)$ and $T(\sigma) = \beta(\sigma)^{-1}$ as functions of σ , with which the data points $(T(\sigma), -\frac{\ell(\sigma, \gamma(\sigma))}{\beta(\sigma)})$ for the free energy can be generated. First, the plot of the free energy as a function of T for representative $(\tilde{\mathcal{J}}/\mathcal{J})^2$ is shown in figure 12. In figure 13, we plot the phase diagram of for representative $(\tilde{\mathcal{J}}/\mathcal{J})^2$ with $q = 96$. Clearly, we can see that the phase transition exists for smaller $\hat{\mu}$ and T for sufficiently large $\tilde{\mathcal{J}}$. However, as we decrease $\tilde{\mathcal{J}}$ finally the phase transition disappears for any $\hat{\mu}$ and \mathcal{J} (in the example of $q = 96, \hat{\mu} = 0.36$ and $\mathcal{J} = 1$ in figure 12 the phase transition does not exist for $(\tilde{\mathcal{J}}/\mathcal{J})^2 = 0.4$). In figure 14, we show the phase boundaries $T_{c,2BH}$ and

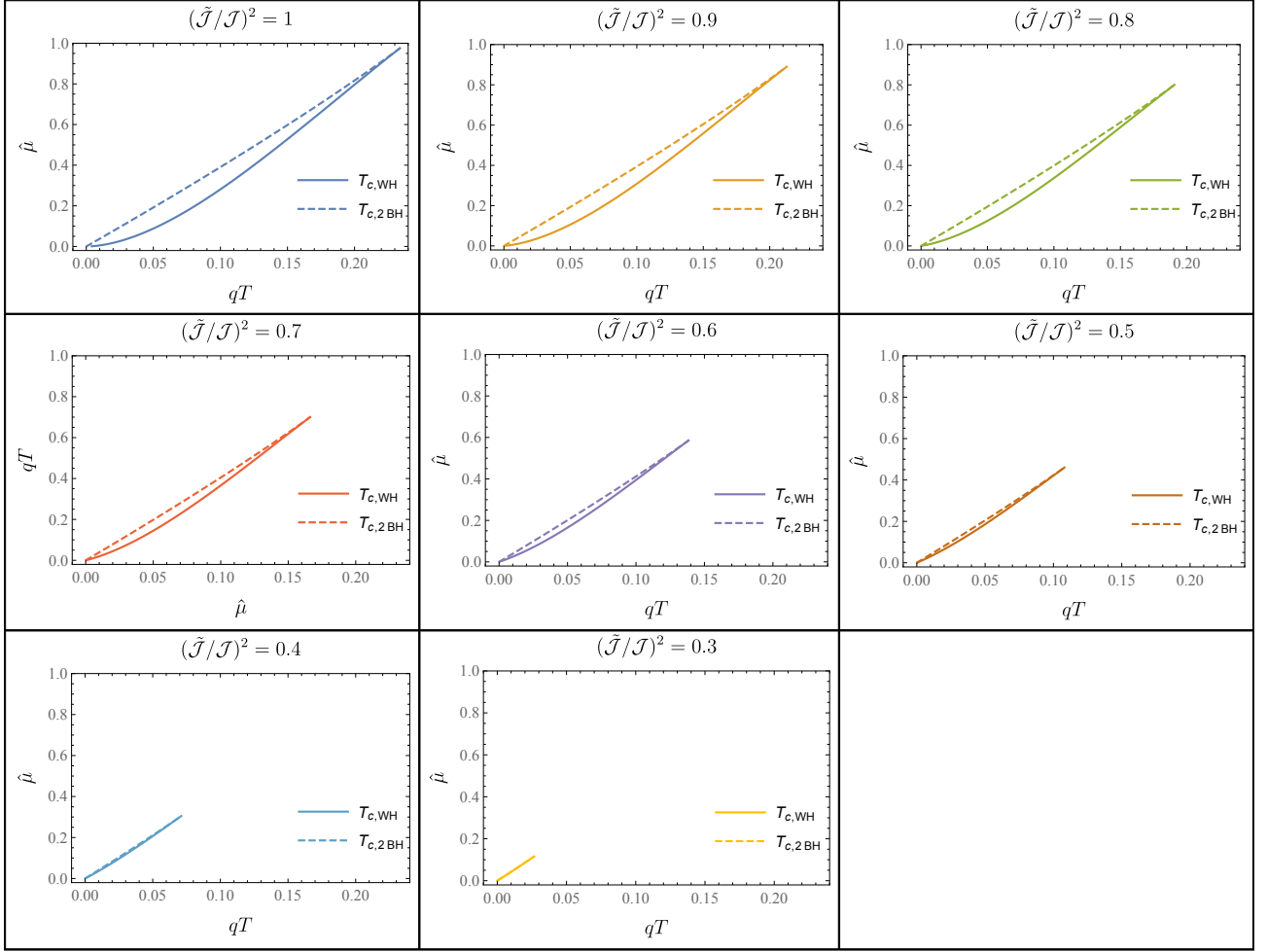


Figure 13: The plots of phase diagrams for representative $\tilde{\mathcal{J}}$.

$T_{c,WH}$ for the same $\tilde{\mathcal{J}}$ simultaneously. We see that the power of $T_{c,2BH}$ is not changed much but $T_{c,WH}$ becomes more straight for smaller $\tilde{\mathcal{J}}$.

The phase transition is replaced by crossover at $\mu = \mu_*$ where $T_{c,2BH}$ and $T_{c,WH}$ meet in the phase diagrams. We call this temperature T_* . These are functions of $\tilde{\mathcal{J}}/\mathcal{J}$. We plot μ_* and T_* as a function in $\tilde{\mathcal{J}}/\mathcal{J}$ in figure 15. In particular, $\mu_* = 0$, or phase transition itself entirely disappears when $\tilde{\mathcal{J}} \approx 0.50\mathcal{J}$ for $q = 96$. For smaller $\tilde{\mathcal{J}}$ the phase transition do not exists for all μ and we only see the crossover. In particular, even at large q limit the phase transition disappears at finite $\tilde{\mathcal{J}}/\mathcal{J}$.

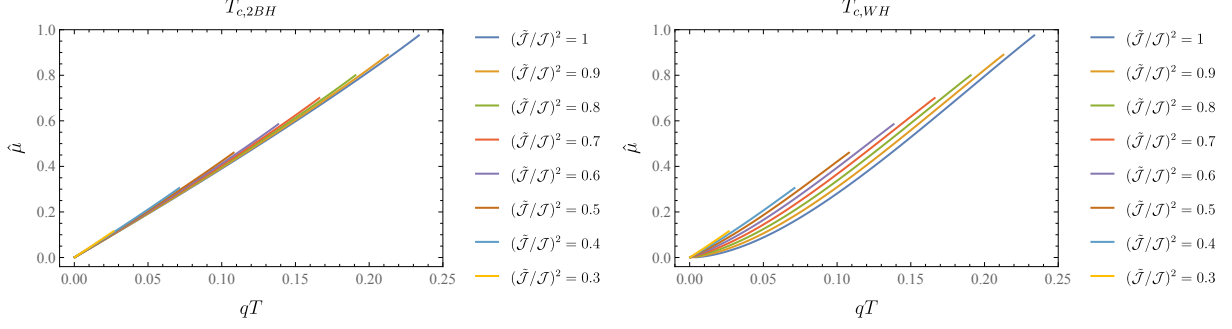


Figure 14: Plots of $T_{c,2BH}$ and $T_{c,WH}$. The parameters are taken to be $\mathcal{J} = 1$, $q = 96$.

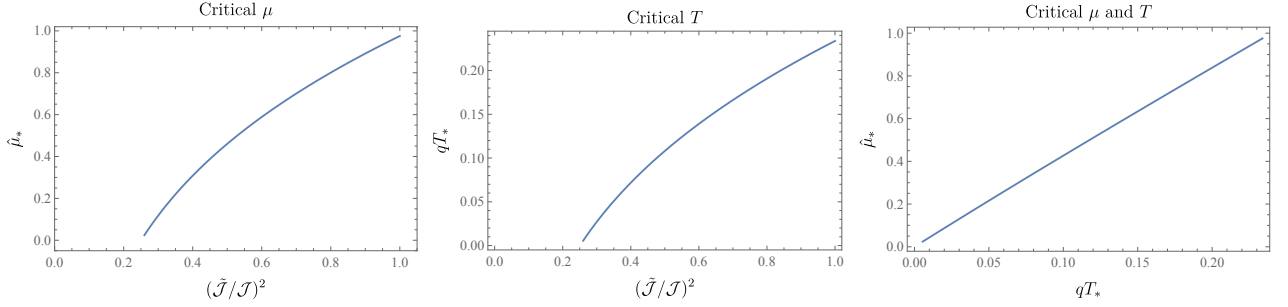


Figure 15: Plots of T_* and μ_* . The parameters are taken to be $\mathcal{J} = 1$, $q = 96$. **Left:** Plot of critical μ as a function of $\tilde{\mathcal{J}}/\mathcal{J}$. **Middle:** Plot of critical T as a function of $\tilde{\mathcal{J}}/\mathcal{J}$. **Right:** Parametric plot of $T_*(\tilde{\mathcal{J}}/\mathcal{J})$ and $\mu_*(\tilde{\mathcal{J}}/\mathcal{J})$.

4.3 Absence of phase transitions for small $\tilde{\mathcal{J}}/\mathcal{J}$.

Let us regard $(\mathcal{J}, \tilde{\mathcal{J}}, \hat{\mu}, \sigma)$ as fundamental variables instead of $(\mathcal{J}, \tilde{\mathcal{J}}, \hat{\mu}, T)$ and express T as a function of σ (and $\mathcal{J}, \tilde{\mathcal{J}}, \hat{\mu}$) as explained above. When $(\tilde{\mathcal{J}}/\mathcal{J})^2$ is sufficiently large and $\hat{\mu}$ is sufficiently small, $T(\sigma)$ is not a monotonic function of σ , hence a single point in T - μ plane may correspond to several different values of σ . On such a point, different phases corresponding to each value of σ coexist together. On the other hand, when $T(\sigma)$ is monotonic, there are no phase transitions since $\ell(\sigma)$ is a smooth function and hence the free energy F is a smooth function of the temperature T .

Now we study the monotonicity of $\beta(\sigma)$. The derivative becomes

$$\frac{d\beta}{d\sigma} \equiv \frac{d\beta(\gamma(\sigma), \sigma)}{d\sigma} = \frac{q}{\hat{\mu}} \tanh \tilde{\gamma} \left(\frac{\log \frac{q}{\sigma}}{\sinh \tilde{\gamma} \cosh \tilde{\gamma} + \tanh \gamma} - \frac{1}{\sigma} \right). \quad (4.27)$$

Here we used the chain rule $\frac{d\beta}{d\sigma} = \frac{d\gamma}{d\sigma} \frac{\partial \beta}{\partial \gamma} + \frac{\partial \beta}{\partial \sigma}$, together with $\frac{d\gamma(\sigma)}{d\sigma} = -\frac{\tanh \gamma}{\sinh \tilde{\gamma} \cosh \tilde{\gamma} + \tanh \gamma}$ which follows from the relation $\hat{\mu} = 2\mathcal{J} \sinh \gamma \tanh \tilde{\gamma}$ (4.24). Here we take the σ derivative while

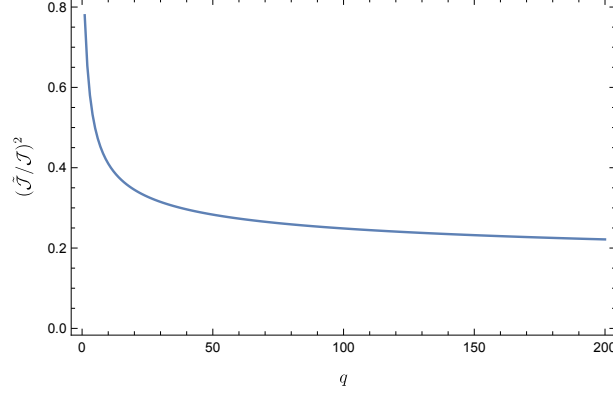


Figure 16: The critical value of $(\tilde{\mathcal{J}}/\mathcal{J})^2$ in the large q approximation where the phase transition becomes a smooth crossover in the entire $(\hat{\mu}, T)$ -plane.

keeping $\hat{\mu}$. For $\tilde{\mathcal{J}} = \mathcal{J}$, which is the equal coupling in left and right, (4.27) is not monotonic for sufficiently small $\hat{\mu}$ and show the first order phase transition. In figure 13, we have observed that as $\tilde{\mathcal{J}}/\mathcal{J}$ is decreased, μ_* , the critical value of μ where the phase transition disappears becomes smaller. When $\tilde{\mathcal{J}}/\mathcal{J}$ crosses some critical value, μ_* finally reaches zero, where the phase transition completely disappears on the (μ, T) -plane. To determine this critical value of $\tilde{\mathcal{J}}/\mathcal{J}$ as a function of q , let us consider the limit $\hat{\mu} \rightarrow 0$, which gives us

$$\gamma(\sigma) \approx \frac{\hat{\mu}}{2\mathcal{J} \tanh(s + \sigma)}, \quad \frac{d\beta}{d\sigma} \approx \frac{q}{2\hat{\mu}\sigma \cosh^2(s + \sigma)} \left(\frac{2\sigma \log \frac{q}{\sigma}}{1 + \frac{\hat{\mu}}{\sinh^2(s + \sigma)}} - \sinh(2s + 2\sigma) \right). \quad (4.28)$$

We are interested only in whether $\frac{d\beta}{d\sigma}$ flips its sign or not. Writing $\frac{d\beta}{d\sigma}$ in the following form

$$\frac{d\beta}{d\sigma} = (\text{positive}) \times (2\sigma \log \frac{q}{\sigma} - \sinh(2s + 2\sigma)), \quad (4.29)$$

we find that the last factor is negative at $\sigma \rightarrow 0, \infty$ and gain its maximum at some finite σ_* where $\frac{d}{d\sigma}(\frac{d\beta}{d\sigma})|_{\sigma_*} = 0$, which is given by

$$2 \log \frac{q}{\sigma_*} - 2 - 2 \cosh(2s + 2\sigma_*) = 0. \quad (4.30)$$

Hence the critical value of $(\tilde{\mathcal{J}}/\mathcal{J})^2$ is determined by the condition $\frac{d\beta}{d\sigma}|_{\sigma_*} = 0$. Solving this condition numerically we obtain figure 16. In particular, when $q = 96$ we obtain $\tilde{\mathcal{J}}/\mathcal{J} = 0.500577$, which is consistent with the critical value we have observed in the previous section.

If we further consider the case $\tilde{\mathcal{J}} \ll \mathcal{J}$, i.e., $s \gg 1$, the condition (4.30) and for σ_* reduces to $\log \frac{q}{\sigma_*} \approx \frac{1}{2}e^{2s}$, and the condition $\frac{d\beta}{d\sigma}|_{\sigma_*} = 0$ gives the critical value of $(\tilde{\mathcal{J}}/\mathcal{J})^2$ as

$$\left(\frac{\tilde{\mathcal{J}}}{\mathcal{J}} \right)^2 \approx \frac{1}{2 \log(2q)}. \quad (4.31)$$

This result also suggests that the phase transition remains at $q = \infty$ limit as far as the $J_{i_1 \dots i_q}^{(L)}$ and $J_{i_1 \dots i_q}^{(R)}$ are correlated even slightly.

The derivative of ℓ is

$$\begin{aligned} \frac{d\ell}{d\sigma} &= \left(\frac{\log \frac{q}{\sigma}}{\sinh \tilde{\gamma} \cosh \tilde{\gamma} + \tanh \gamma} - \frac{1}{\sigma} \right) \frac{1}{\log \frac{q}{\sigma}} \beta \frac{\partial \ell}{\partial \beta} \\ &= \frac{q}{\hat{\mu} \tanh \tilde{\gamma} \log \frac{q}{\sigma}} \frac{d\beta}{d\sigma} \beta \frac{\partial \ell}{\partial \beta}. \end{aligned} \quad (4.32)$$

Since $\frac{\partial \ell}{\partial \beta} = -E/N$ is always positive from the expression (4.25), $\ell(\sigma)$ is also a monotonic function when $\beta(\sigma)$ is monotonic. Therefore, when $\beta(\sigma)$ is monotonic the free energy F is also a monotonic function of the temperature T .

4.4 Inverse temperature of order $\beta \sim q$ and beyond

First we consider the order of $\beta \sim q$. In this regime, G_{LR} is smaller than $1/2$ even for $\tau \ll q$. Therefore we can put $G_{LR}^q = 0$ for $\tau \gg q$ and the effective decay rate ν becomes the naive one $\nu = \mu$. Matching with the solution with $\tau \ll q$ regime we obtain

$$\alpha = \mathcal{J} \sinh \gamma = \frac{\hat{\mu}}{2} \tanh \frac{\beta \mu}{2} \quad (4.33)$$

The ratio $\tilde{\mathcal{J}}/\mathcal{J}$ do not enter in the correlation function and $\tilde{\mathcal{J}}$ dependence disappears at the order of $\beta \sim q$. Indeed the correlation function and the partition function take the same form both in Maldacena-Qi model [24] and Kourkoulou-Maldacena model [29]. Since the behaviors are exactly the same for any $\tilde{\mathcal{J}}$, we only draw the results from [24, 29] in this paper.

The free energy now becomes

$$-\frac{\beta F}{N} = \log \left(2 \cosh \frac{\beta \mu}{2} \right) + \frac{\beta \mu}{q} \tanh \frac{\beta \mu}{2} \left[\log(2 \sinh \gamma) + \frac{1}{\tanh \gamma} - \gamma - 1 \right] \quad (4.34)$$

This is independent from the ratio $\tilde{\mathcal{J}}/\mathcal{J}$ and does not depend on the incompleteness of the random couplings.

At the order of $\beta \sim \sqrt{q}$, the chaos exponent increases from very small value and finally saturates the chaos bound [24, 29]. The correlation function G_{LR} at this order becomes

$$G_{LR}(\tau) = \frac{i}{2} \mu \left(\frac{\beta}{2} - \tau \right), \quad (4.35)$$

which is of order $1/\sqrt{q}$. The free energy is

$$-\frac{\beta F}{N} = \log 2 + \frac{(\beta \mu)^2}{8} + \frac{2\beta \mathcal{J}}{q^2} + \frac{(\beta \mu)^2}{2q} \log(\beta \mathcal{J}) + \frac{h[q(\beta \mu)^2]}{q^2}. \quad (4.36)$$

where h is a function that we have not determined.

At the order of $\beta \sim 1$, we can set $\mu = 0$ to compute g_{LL}, g_{RR} and we recover the decoupled SYK models at large q limit. The free energy is

$$\frac{F}{N} = \frac{2F_{SYK}}{N} - \frac{\beta\mu^2}{8}, \quad (4.37)$$

where F_{SYK} is the free energy of the SYK.

4.4.1 Comments on subleading Lyapunov exponents

At finite q , we find that there is a subleading Lyapunov exponents in the $\sigma = -1$ sector. In the large q perspective, the problem to find Lyapunov exponents reduces to studying the bound states of a Schrödinger equation, and we can understand the subleading Lyapunov exponents using that language as follows. At $\mu = 0$ we have two copies of the SYK and the Lyapunov exponents are degenerate. After introducing μ , two degeneracies are resolved and we will get two different exponents, which leads to the subleading Lyapunov exponents.

However, at leading order of $1/q$ expansion, the degeneracy is not resolved because σ dependent term is actually of order $1/q$ at large q limit. By taking the large q limit of (3.16), we obtain

$$\begin{aligned} M_{1,LLLL}(t) &\propto (G_{LL}^R)^2 = O(1), & M_{1,LLLR}(t) &\propto G_{LL}^R G_{LR}^R = O(1/\sqrt{q}), \\ M_{1,LRLR}(t) &\propto (G_{LR}^R)^2 = O(1/q), & M_{2,LL}(t) &= -2\mathcal{J}^2 e^{g_{LL}(\beta/2+it)}, & M_{2,LR}(t) &= 0. \end{aligned} \quad (4.38)$$

where we have used the fact that G_{LR} is of order $1/\sqrt{q}$. Therefore the only surviving term at large q is $M_{1,LLLL}(t)$ and $M_{2,LL}(t)$ and we find that σ dependent terms drop at the leading of $1/q$ expansion. This means that what we get is the degenerate Lyapunov exponents at any temperature at large q . We will pose the calculation of the leading correction to see the resolution of the degeneracy.

5 Structure of ground state for imperfectly correlated disorders

In this section we investigate the structure of the ground state of the coupled model (2.1). Let us consider the following state $|I(\beta)\rangle$

$$|I(\beta)\rangle = \frac{1}{\mathcal{N}} e^{-\frac{\beta}{4}(H_{SYK}^{(L)} + H_{SYK}^{(R)})} |I\rangle, \quad (5.1)$$

where $|I\rangle$ is the ground state of $H_{int} = i \sum_{i=1}^N \psi_i^L \psi_i^R$ and $\mathcal{N} = \sqrt{\langle I | e^{-\frac{\beta}{2}(H_{SYK}^{(L)} + H_{SYK}^{(R)})} | I \rangle}$ is the normalization factor. When the correlation of $J_{i_1 \dots i_q}^{(L)}$ and $J_{i_1 \dots i_q}^{(R)}$ is perfect, this state is the thermofield double state. Therefore the state $|I(\beta)\rangle$ is a generalization of the thermofield double state. In the limit $\mu \rightarrow \infty$, the ground state of H approaches $|I(\beta)\rangle$ with $\beta = 0$. Also in the limit $\beta \rightarrow \infty$, $|I(\beta)\rangle$ is approximated with the ground state of $H_{SYK}^{(L)} + H_{SYK}^{(R)}$. If we assume that the ground state of $H_{SYK}^{(L)} + H_{SYK}^{(R)}$ is non-degenerate, it coincides with the ground state of the coupled model in the limit $\mu \rightarrow 0$. Therefore $|I(\beta)\rangle$ should be a good one-parameter ansatz to approximate the ground state of the two-coupled system (2.1) at least in the limit $\mu \rightarrow \infty$ and $\mu \rightarrow 0$. When the two random couplings are perfectly correlated, $|I(\beta)\rangle$ was found to be a good approximation of the ground state also for finite μ [24, 27, 28]. In this appendix we provide some pieces of evidence that $|I(\beta)\rangle$ approximate the ground state for finite μ well even when the correlation between $J_{i_1 \dots i_q}^{(L)}$ and $J_{i_1 \dots i_q}^{(R)}$ is imperfect.

5.1 Variational approximation in large q limit

To understand the ground state of imperfect left-right coupling model, here we study the variational approximation by the generalized thermofield double state

$$|I(\beta)\rangle = \frac{1}{\sqrt{Z_{LR}}} e^{-\frac{\beta}{4}H_L} e^{-\frac{\beta}{4}H_R} |I\rangle. \quad (5.2)$$

Here the $|I\rangle$ is the maximally entangled state defined by

$$\psi_L^i |I\rangle = -i\psi_R^i |I\rangle. \quad (5.3)$$

This is the ground state of the coupling Hamiltonian $H_{int} = -i\mu \sum_{i=1}^N \psi_L^i \psi_R^i$. Z_{LR} is the normalization factor defined by

$$Z_{LR} = \langle I | e^{-\frac{\beta}{2}H_L} e^{-\frac{\beta}{2}H_R} | I \rangle = \text{Tr}(e^{-\frac{\beta}{2}H_L} e^{-\frac{\beta}{2}H_R}). \quad (5.4)$$

In Maldacena-Qi model, choosing the appropriate β , $|I(\beta)\rangle$ is a very good approximation for the exact ground state in the sense that the leading term of the overlap between them becomes 1 in small μ or in the large q limit. In Kourkoulou-Maldacena model, this state is still a good approximation in the sense that the leading overlap is 1 at large q . Therefore, we expect that the state $|I(\beta)\rangle$ is a good approximation for the exact ground state even when the correlation of left right coupling is imperfect.

We study the variational approximation by $|I(\beta)\rangle$ at large q . To do that, we minimize the trial energy

$$E_{\text{trial}}(\beta) = \langle I(\beta) | H_L + H_R + H_{int} | I(\beta) \rangle. \quad (5.5)$$

In terms of the Euclidean correlation functions on the thermal circle with interfaces which are schematically depicted in figure 17, the trial energy is

$$\langle H_L + H_R + H_{int} \rangle_{|I(\beta)\rangle} = \frac{1}{q} \partial_\tau G_{LL}(\tau, 0) \Big|_{\tau \rightarrow 0_+} + \frac{1}{q} \partial_\tau G_{LR}(\tau, 0) \Big|_{\tau \rightarrow 0_+} + i\mu G_{LR}(0, 0). \quad (5.6)$$

At large q limit, the correlation function becomes $G_{\alpha\beta}(\tau_1, \tau_2) = G_{0,\alpha\beta} \left(1 + \frac{1}{q} g_{\alpha\beta}(\tau_1, \tau_2) \right)$ with [40, 41]

$$\begin{aligned} e^{g_{LL}(\tau_1, \tau_2)} = e^{g_{RR}(\tau_1, \tau_2)} &= \left(\frac{\check{\alpha}}{\mathcal{J} \sin(\check{\alpha}|\tau_1 - \tau_2| + \check{\gamma})} \right)^2, \quad \text{for} \quad -\frac{\beta}{4} < \tau_1, \tau_2 < \frac{\beta}{4}, \\ e^{g_{LR}(\tau_1, \tau_2)} &= \left(\frac{\check{\alpha}^2 / \mathcal{J}^2}{-\lambda^2 \sin(\check{\alpha}(\tau_1 + \frac{\beta}{4})) \sin(\check{\alpha}(\tau_2 - \frac{\beta}{4})) + \sin(\check{\alpha}(\frac{\beta}{4} - \tau_1) + \check{\gamma}) \sin(\check{\alpha}(\frac{\beta}{4} - \tau_2) + \check{\gamma})} \right)^2, \\ &\quad \text{for} \quad -\frac{\beta}{4} < \tau_1, \tau_2 < \frac{\beta}{4}. \end{aligned} \quad (5.7)$$

Here we introduced a parameter $\lambda = \tilde{\mathcal{J}}/\mathcal{J}$. The parameters $\check{\alpha}$ and $\check{\gamma}$ satisfy

$$\check{\alpha} = \mathcal{J} \sin \check{\gamma}, \quad \sin \left(\frac{\check{\alpha}\beta}{2} + 2\check{\gamma} \right) = \lambda^2 \sin \left(\frac{\check{\alpha}\beta}{2} \right). \quad (5.8)$$

Then, $E_{\text{trial}}(\beta)$ becomes

$$E_{\text{trial}}(\beta) = -\frac{2\mathcal{J}}{q^2} \cos \check{\gamma} - \frac{\hat{\mu}}{2q} - \frac{\hat{\mu}}{q^2} \log \left[\frac{\sin^2 \check{\gamma}}{(1 - \lambda^2) + \sqrt{(1 - \lambda^2)^2 + 4\lambda^2 \sin^2 \check{\gamma}}} \right]. \quad (5.9)$$

Here we used the relation

$$\begin{aligned} \frac{1}{q} \partial_\tau G_{LL}(\tau, 0) \Big|_{\tau \rightarrow 0_+} &= -\frac{\mathcal{J}}{q^2} \cos \check{\gamma}, \\ e^{g_{LR}(0,0)} &= \left(\frac{\check{\alpha}^2 / \mathcal{J}^2}{-\lambda^2 \sin^2 \frac{\check{\alpha}\beta}{4} + \sin^2(\frac{\check{\alpha}\beta}{4} + \check{\gamma})} \right)^2 = \left(\frac{2 \sin^2 \check{\gamma}}{(1 - \lambda^2) + \sqrt{(1 - \lambda^2)^2 + 4\lambda^2 \sin^2 \check{\gamma}}} \right)^2 \end{aligned} \quad (5.10)$$

Because of the chain rule, we can instead take the derivative w.r.t. $\check{\gamma}$ to minimize the trial energy:

$$q^2 \frac{\partial E_{\text{trial}}}{\partial \check{\gamma}} = 2\mathcal{J} \sin \check{\gamma} - \frac{\hat{\mu}}{\tan \check{\gamma}} \frac{(1 - \lambda^2) + \sqrt{(1 - \lambda^2)^2 + 4\lambda^2 \sin^2 \check{\gamma}}}{\sqrt{(1 - \lambda^2)^2 + 4\lambda^2 \sin^2 \check{\gamma}}} = 0. \quad (5.11)$$

This equation is solved as

$$\cos \check{\gamma} = \cosh \gamma - \sinh \gamma \tanh \tilde{\gamma}, \quad (5.12)$$

where γ is the solution of the equation (4.8). This determines the variational parameter β as a function of μ .

We find that the SYK energy and the expectation value of the interaction Hamiltonian completely agree:

$$\langle H_L + H_R \rangle_{|G(\mu)\rangle} = \langle H_L + H_R \rangle_{|I(\beta(\mu))\rangle} = -\frac{2\mathcal{J}}{q^2} \cos \check{\gamma}$$

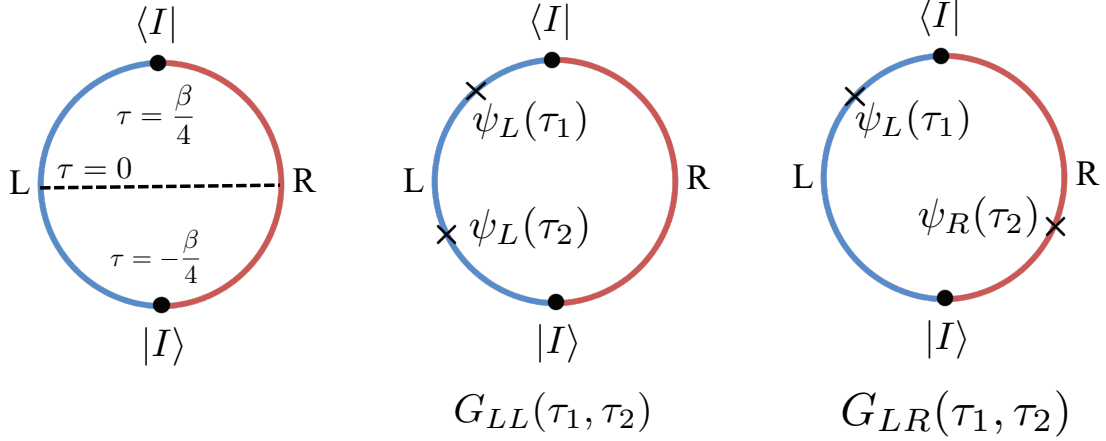


Figure 17: The schematic pictures of the correlation functions. **Left:** The path integral representation for the partition function Z_{LR} . **Middle:** The correlation function G_{LL} . **Right:** The correlation function G_{LR} .

$$\langle \psi_L \psi_R \rangle_{|G(\mu)\rangle} = \langle \psi_L \psi_R \rangle_{|I(\beta(\mu))\rangle} = \frac{i}{2} \left[1 + \frac{1}{q} \log \left(\frac{e^s \sinh \gamma}{\cosh \tilde{\gamma}} \right)^2 \right] \quad (5.13)$$

Therefore, the variational energy actually is equal to the true energy (4.25)

$$E_{\text{trial}}(\beta(\mu)) = E_g. \quad (5.14)$$

This means that the $|I(\beta(\mu))\rangle = |G(\mu)\rangle$ in the large q limit.

5.2 Overlap between ground state and $|I(\beta)\rangle$ for finite q

In the previous section we have found that $|I(\beta)\rangle$ (5.1), with $\beta(\mu)$ chosen appropriately, approximate the energy of the ground state well when both q and N are large. This is a strong evidence that $|I(\beta)\rangle$ approximate well the true ground state $|gs\rangle$ of the two-coupled Hamiltonian (2.1). In this appendix we study the validity of this approximation for finite q by comparing the two states directly for finite N .

Note that there are several subtleties. First, since the full Hamiltonian as well as $i \sum_{i=1}^N \psi_i^L \psi_i^R$ commute with the fermion number parity Γ_c (B.4), both $|I(\beta)\rangle$ and the ground state of H are eigenstates of Γ_c . When μ is not sufficiently large, the parity of the ground state of H depends on the realization of $J_{i_1 \dots i_q}^{(a)}$ and hence not always the same as the parity of $|I(\beta)\rangle$. Hence to make the comparison reasonable we should compare $|I(\beta)\rangle$ with $|gs, (-1)^{\frac{N(N-1)}{2}}\rangle$, the eigenstate of H with the lowest energy in the same parity sector as $|I(\beta)\rangle$, $\Gamma_c = (-1)^{\frac{N(N-1)}{2}}$, rather than the true ground state of H .

Second, although $|I(\beta)\rangle$ approximate well the ground state at $\mu \approx 0$ when the ground state of $H_{SYK}^{(L)} + H_{SYK}^{(R)}$ is non-degenerate, the spectrum of single SYK Hamiltonian has the following degeneracy depending of the value of q and $N \bmod 8$ [42]:

| q, N | degeneracy of single SYK spectrum |
|---|--------------------------------------|
| $q = 0 \bmod 4, \quad N = 2, 6 \bmod 8$ | 2 (between different parity sectors) |
| $q = 0 \bmod 4, \quad N = 4 \bmod 8$ | 2 (in each parity sector) |
| $q = 0 \bmod 4, \quad N = 0 \bmod 8$ | non-degenerate |
| $q = 2 \bmod 4$ | non-degenerate |

(5.15)

which implies that the ground state of $H_{SYK}^{(L)} + H_{SYK}^{(R)}$ is also degenerate in the cases of the first two rows. On the other hand, $|I\rangle$ contains only the certain linear combination of them (which can be identified explicitly for $J_{i_1 \dots i_q}^{(L)} = J_{i_1 \dots i_q}^{(R)}$ case, as summarized in appendix B). Note that this degeneracy cannot be removed completely by the total fermion number parity $(-1)^F$. When μ is small but non-zero, the degeneracy is removed and the true ground state is approximately a certain linear combination of the degenerate ground states at $\mu = 0$. This linear combination varies depending on the realization of $J_{i_1 \dots i_q}^{(a)}$ and is not necessarily the same as the linear combination contained in $|I\rangle$.

To avoid these subtleties, here we choose $q = 6$ where the ground state in $\Gamma_c = (-1)^{\frac{N(N-1)}{2}}$ sector at $\mu = 0$ is non-degenerate for any N , and consider the overlap between $|I(\beta)\rangle$ and $|gs, (-1)^{\frac{N(N-1)}{2}}\rangle$, maximized with respect to β . As a result we obtain figure 18. The results suggest that $|I(\beta)\rangle$ is indeed a good approximation to $|gs, (-1)^{\frac{N(N-1)}{2}}\rangle$ also for finite μ .

6 Discussion and Future works

In this paper we have studied the thermodynamic and chaotic properties of the two-coupled SYK model where the two random couplings are not completely the same. As a result we have found that the phase transition temperature becomes smaller as the correlation of the random couplings is reduced. This is consistent with the intuition that the correlation of between the random couplings make it easier for the wormhole to form between the two sites.

Then, we studied the ground state properties of the coupled SYK with imperfect correlations of the random couplings. As we change the left right correlation, the behavior of the energy gap also changes. When $\tilde{\mathcal{J}}/\mathcal{J}$ is close to 1, the SYK interaction still helps to make the gap larger than the naive one μ . However as we decrease μ , finally the effect of imperfect left right correlation wins and the energy gap becomes smaller than the naive one, which we expect when we have no correlation between left and right. For $\tilde{\mathcal{J}}$ where the thermal phase transition disappears, the energy gap is close to that without left and right correlation as far as we checked.

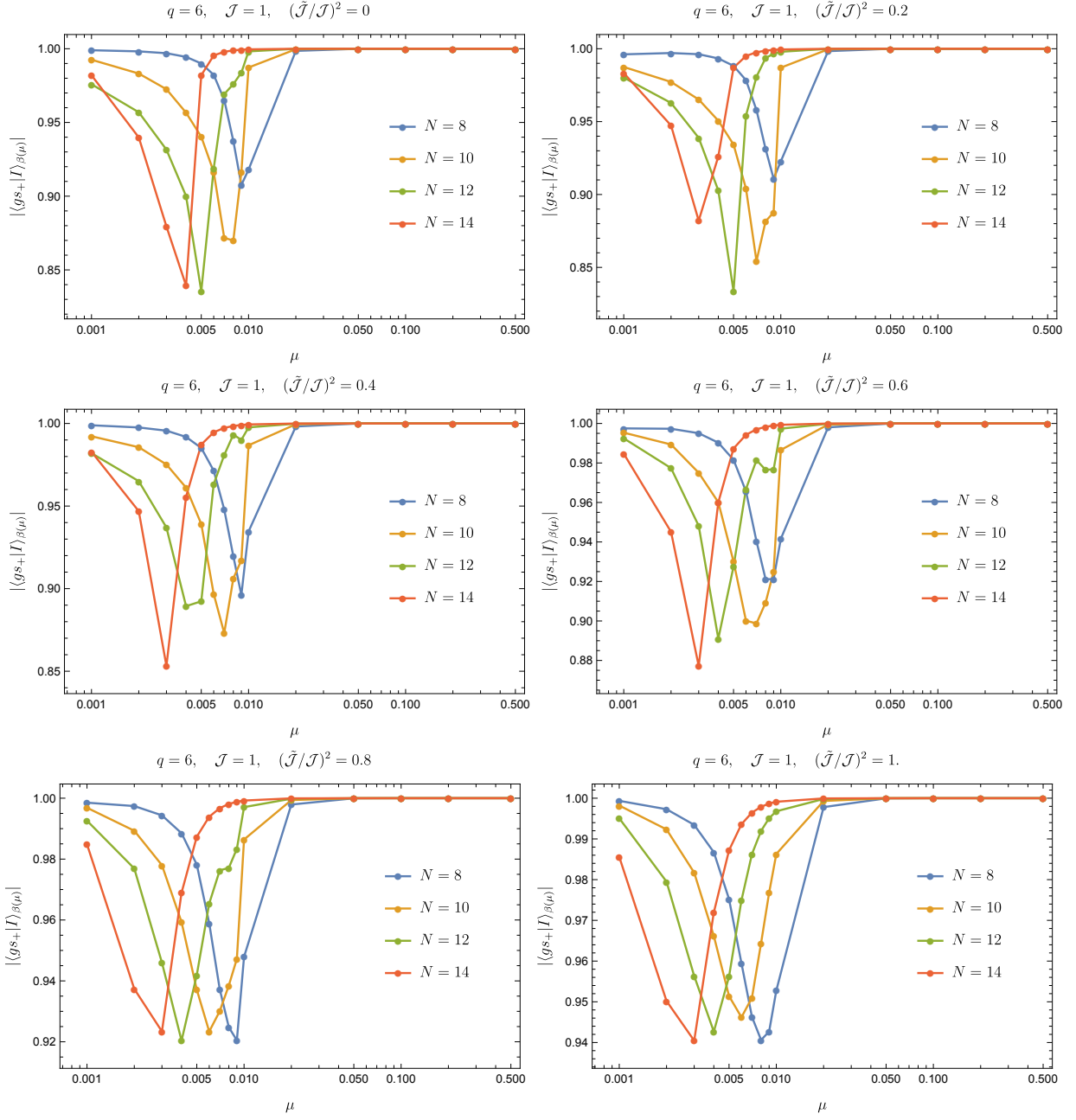


Figure 18: The overlap $|\langle I_\beta | gs, (-1)^{\frac{N(N-1)}{2}} \rangle|$ maximized with respect to β .

We have also found that the transmission amplitude between two SYK sites in the wormhole phase for fixed temperature T and the direct LR coupling μ becomes smaller as the correlation of the random couplings is reduced. On the other hand, as the correlation is reduced the largest chaos exponent becomes larger. Assuming that the largest chaos exponent is associated with the information spreading within each site rather than between the two sites, this behavior of the chaos exponent is also consistent with the same intuition. Interestingly, we have also found that the phase transition completely disappears when the correlation between the random couplings is smaller than some non-zero finite value which is around $\langle J_{i_1 \dots i_q}^{(L)} J_{i_1 \dots i_q}^{(R)} \rangle \approx 0.3 \langle (J_{i_1 \dots i_q}^{(L)})^2 \rangle$ for $q = 4$ and $\langle J_{i_1 \dots i_q}^{(L)} J_{i_1 \dots i_q}^{(R)} \rangle \sim (\log q)^{-1} \langle (J_{i_1 \dots i_q}^{(L)})^2 \rangle$ for large q .

Finally, to understand the properties of the ground state, we studied how it is close to the generalized thermofield double state. This generalized thermofield double state has a jump of couplings in Euclidean time and studied in the context of black holes [19, 21, 20, 23]. It turns out that the ground state coincides with the generalized thermofield double state at large q . In that sense, the coupled Hamiltonian prepare an ‘‘SYK Janus black holes’’ as its ground state. In the case of SYK Janus black holes, we have an expanded interiors. Intuitively, this expanded interior makes the length between two mouths of the wormholes longer and it takes much time to traverse the wormhole. This is an intuitive explanation of why the E_{gap} , which is roughly the time to traverse the wormhole, becomes larger for smaller $\tilde{\mathcal{J}}/\mathcal{J}$.

In section 3.3.2 we have found that the ladder kernel for the four point functions can be block-diagonalized into two sectors labelled by $\sigma = \pm 1$, and have observed that the chaos exponent in the $\sigma = -1$ sector vanishes at some temperature $T = T_{c, \text{Ly}}(\mu, \tilde{\mathcal{J}}/\mathcal{J})$ which is larger than $T_{c, \text{WH}}$ (the vanishing chaos exponent was also observed in [30] for $J_{i_1 \dots i_q}^{(L)} = J_{i_1 \dots i_q}^{(R)}$). It would be interesting to investigate the physical interpretation of this phenomenon. For this purpose it would be important to reproduce the same phenomenon analytically in the large q limit. As commented in section 4.4.1 this requires the analysis of the sub-leading correction in $1/q$.

Acknowledgement

We thank Kanato Goto, Cheng Peng, Dario Rosa and Yingyu Yang for valuable discussions and useful comments. The numerical analyses in this paper were performed on sushiki server in Yukawa Institute Compute Facility and on Ulysses cluster v2 in SISSA. TN is supported by MEXT KAKENHI Grant-in-Aid for Transformative Research Areas A ‘‘Extreme Universe’’ Grant Number 22H05248.

A A derivation of the large q partition function

The solution for $\tau \ll q$ is

$$\begin{aligned} e^{g_{LL}(\tau)} &= \frac{\alpha^2}{\mathcal{J}^2 \sinh^2(\alpha|\tau| + \gamma)}, \\ e^{g_{LR}(\tau)} &= \frac{\tilde{\alpha}^2}{\tilde{\mathcal{J}}^2 \cosh^2(\tilde{\alpha}|\tau| + \tilde{\gamma})}, \end{aligned} \quad (\text{A.1})$$

and for $\tau \gg q$

$$\begin{aligned} G_{LL}(\tau) &= A \cosh \left[\nu \left(\frac{\beta}{2} - \tau \right) \right], \\ G_{LR}(\tau) &= iA \sinh \left[\nu \left(\frac{\beta}{2} - \tau \right) \right]. \end{aligned} \quad (\text{A.2})$$

where

$$\nu = i \int_{-\infty}^{\infty} \Sigma_{LR}(\tau) d\tau = \frac{2\tilde{\alpha}}{q} = \frac{\hat{\mu}}{q \tanh \tilde{\gamma}}. \quad (\text{A.3})$$

In the matching region, G_{LL} and G_{LR} is expanded as

$$\begin{aligned} G_{LL} &\sim \frac{1}{2} - \frac{1}{q} \left(\log \frac{\mathcal{J}}{\alpha} + \gamma + \alpha\tau \right) \sim A \left[\cosh \frac{\nu\beta}{2} - \tau\nu \sinh \frac{\nu\beta}{2} \right] \\ -iG_{LR} &\sim \frac{1}{2} - \frac{1}{q} \left(\log \frac{\tilde{\mathcal{J}}}{\tilde{\alpha}} + \tilde{\gamma} + \tilde{\alpha}\tau \right) \sim A \left[\sinh \frac{\nu\beta}{2} - \tau\nu \cosh \frac{\nu\beta}{2} \right]. \end{aligned} \quad (\text{A.4})$$

This determines the parameters to be

$$\alpha = \tilde{\alpha}, \quad \tilde{\gamma} = \gamma + \sigma + s, \quad (\text{A.5})$$

Here we defined σ by

$$\sigma = qe^{-\beta\nu}, \quad (\text{A.6})$$

which is of order $O(1)$. The boundary conditions at $\tau = 0$ gives

$$\alpha = \mathcal{J} \sinh \gamma, \quad \hat{\mu} = 2\tilde{\alpha} \tanh \tilde{\gamma}. \quad (\text{A.7})$$

The conditions (A.5), (A.6) and (A.7) determines the relation between the physical parameters $\hat{\mu}, \mathcal{J}, \tilde{\mathcal{J}}, \beta$ and σ, γ, s . The energy is

$$\begin{aligned} \frac{E}{N} &= -\frac{1}{N} \partial_{\beta} \log Z = \frac{1}{2q} \partial_{\tau} g_{LL}(0) + \frac{1}{2q} \partial_{\tau} g_{RR}(0) + i\mu \left(1 - \frac{2}{q} \right) \frac{i}{2} \left(1 + \frac{1}{q} g_{LR}(0) \right) \\ &= -\frac{2\mathcal{J}}{q^2} \cosh \gamma - \frac{\hat{\mu}}{2q} + \frac{\hat{\mu}}{q^2} \left(1 + \log \frac{e^s \sinh \gamma}{\cosh \tilde{\gamma}} \right). \end{aligned} \quad (\text{A.8})$$

In the following we choose the fundamental variables as either $(\hat{\mu}, \mathcal{J}, s, \beta)$ or $(\sigma, \gamma, s, \beta)$ interchangeably. Using the effective action we can write⁴

$$\begin{aligned}\mathcal{J} \frac{\partial \ell}{\partial \mathcal{J}} \Big|_{\hat{\mu}, s, \beta} &= \beta \int_0^\infty (\mathcal{J}^2 e^{g_{LL}} + \tilde{\mathcal{J}}^2 e^{g_{LR}}) d\tau = \frac{\beta \hat{\mu}}{q^2} \left[\frac{1}{\tanh \gamma \tanh \tilde{\gamma}} - 1 \right], \\ \mu \frac{\partial \ell}{\partial \hat{\mu}} \Big|_{\mathcal{J}, s, \beta} &= -i\beta \mu G_{LR}(0) = \frac{\beta \hat{\mu}}{q^2} \left[\frac{q}{2} + \log \left(\frac{\sinh \gamma}{\cosh \tilde{\gamma}} \right) + s \right]\end{aligned}\quad (\text{A.9})$$

By changes of variables, partial derivatives are given by

$$\begin{aligned}\frac{1}{\hat{\mu}} \frac{\partial \hat{\mu}}{\partial \gamma} \Big|_{\sigma, s, \beta} - \frac{1}{\mathcal{J}} \frac{\partial \mathcal{J}}{\partial \gamma} \Big|_{\sigma, s, \beta} &= \frac{1}{\tanh \gamma} + \frac{1}{\sinh \tilde{\gamma} \cosh \tilde{\gamma}}, & \frac{1}{\beta \hat{\mu}} \frac{\partial(\beta \hat{\mu})}{\partial \gamma} \Big|_{\sigma, s, \beta} &= \frac{1}{\sinh \tilde{\gamma} \cosh \tilde{\gamma}}, \\ \frac{1}{\hat{\mu}} \frac{\partial \hat{\mu}}{\partial \sigma} \Big|_{\gamma, s, \beta} - \frac{1}{\mathcal{J}} \frac{\partial \mathcal{J}}{\partial \sigma} \Big|_{\gamma, s, \beta} &= \frac{1}{\sinh \tilde{\gamma} \cosh \tilde{\gamma}}, & \frac{1}{\beta \hat{\mu}} \frac{\partial(\beta \hat{\mu})}{\partial \sigma} \Big|_{\gamma, s, \beta} &= \frac{1}{\sinh \tilde{\gamma} \cosh \tilde{\gamma}} - \frac{1}{\sigma \log \frac{q}{\sigma}}\end{aligned}\quad (\text{A.10})$$

Then, the derivative of ℓ in γ, σ is determined through

$$\begin{aligned}\frac{\partial \ell}{\partial \gamma} \Big|_{\sigma, s, \beta} &= \frac{1}{\beta \hat{\mu}} \frac{\partial(\beta \hat{\mu})}{\partial \gamma} \Big|_{\sigma, s, \beta} \beta \frac{\partial \ell}{\partial \beta} \Big|_{\hat{\mu}, \mathcal{J}, s} - \left(\frac{1}{\hat{\mu}} \frac{\partial \hat{\mu}}{\partial \gamma} \Big|_{\sigma, s, \beta} - \frac{1}{\mathcal{J}} \frac{\partial \mathcal{J}}{\partial \gamma} \Big|_{\sigma, s, \beta} \right) \mathcal{J} \frac{\partial \ell}{\partial \mathcal{J}} \Big|_{\hat{\mu}, s, \beta} \\ \frac{\partial \ell}{\partial \sigma} \Big|_{\gamma, s, \beta} &= \frac{1}{\beta \hat{\mu}} \frac{\partial(\beta \hat{\mu})}{\partial \sigma} \Big|_{\gamma, s, \beta} \beta \frac{\partial \ell}{\partial \beta} \Big|_{\hat{\mu}, \mathcal{J}, s} - \left(\frac{1}{\hat{\mu}} \frac{\partial \hat{\mu}}{\partial \sigma} \Big|_{\gamma, \beta, s} - \frac{1}{\mathcal{J}} \frac{\partial \mathcal{J}}{\partial \sigma} \Big|_{\gamma, \beta, s} \right) \mathcal{J} \frac{\partial \ell}{\partial \mathcal{J}} \Big|_{\hat{\mu}, s, \beta}.\end{aligned}\quad (\text{A.11})$$

Here we used the relation $(\mu \partial_\mu + \mathcal{J} \partial_\mathcal{J} - \beta \partial_\beta) \ell = 0$ since ℓ is a function of dimensionless parameters $\ell(\beta \hat{\mu}, \mathcal{J} \beta, s)$. Integrating (A.11), we obtain

$$\ell(\sigma, \gamma) = \frac{\tanh \tilde{\gamma} \log \frac{q}{\sigma}}{q} \left(\frac{q}{2} - 1 + \frac{1}{\tanh \gamma \tanh \tilde{\gamma}} + \log \frac{\sinh \gamma}{\cosh \tilde{\gamma}} + s + \frac{\sigma}{\tanh \tilde{\gamma}} \right) + \frac{\sigma}{q}, \quad (\text{A.12})$$

which is the result in (4.26). Interestingly, the effect of incomplete correlation $\mathcal{J} \neq \tilde{\mathcal{J}}$ is included in $\tilde{\gamma}$ and the partition function takes the same form with the completely correlated random couplings $\mathcal{J} = \tilde{\mathcal{J}}$.

B Relation between ground state of H_{int} and eigenstates of $H_{SYK}^{(a)}$

In this section we display the explicit relation between $|I\rangle$, the ground state of H_{int} (2.2), and the eigenstates of $H_{SYK}^{(L)} + H_{SYK}^{(R)}$ for $J_{i_1 \dots i_q}^{(L)} = J_{i_1 \dots i_q}^{(R)}$. For $q = 4$ the results are also written in [27].

⁴Here we take the \mathcal{J} derivative with fixed s and $\partial_\mathcal{J}$ also acts on $\tilde{\mathcal{J}}$ terms.

B.1 Gamma matrices and charge conjugation matrix

Let us first fix the convention for the gamma matrices, and also introduce the charge conjugation operator C for single site, which play a crucial role in fixing the ambiguities of the overall phases of the eigenstates of $H_{SYK}^{(L)} + H_{SYK}^{(R)}$.

We choose the representation of the single-site gamma matrices γ_i and single-site fermion number parity matrix γ_c as

$$\begin{aligned}\gamma_1 &= X \otimes 1 \otimes 1 \otimes 1 \otimes \cdots \otimes 1 \otimes 1, \\ \gamma_2 &= Y \otimes 1 \otimes 1 \otimes 1 \otimes \cdots \otimes 1 \otimes 1, \\ \gamma_3 &= Z \otimes X \otimes 1 \otimes 1 \otimes \cdots \otimes 1 \otimes 1, \\ \gamma_4 &= Z \otimes Y \otimes 1 \otimes 1 \otimes \cdots \otimes 1 \otimes 1, \\ \gamma_5 &= Z \otimes Z \otimes X \otimes 1 \otimes \cdots \otimes 1 \otimes 1, \\ &\vdots \\ \gamma_N &= Z \otimes Z \otimes Z \otimes Z \otimes \cdots \otimes Z \otimes Y, \\ \gamma_c &= (-i)^{\frac{N}{2}} \gamma_1 \gamma_2 \cdots \gamma_N = Z^{\otimes \frac{N}{2}},\end{aligned}\tag{B.1}$$

where

$$X = \begin{pmatrix} 0 & 1 \\ 1 & 0 \end{pmatrix}, \quad Y = \begin{pmatrix} 0 & -i \\ i & 0 \end{pmatrix}, \quad Z = \begin{pmatrix} 1 & 0 \\ 0 & -1 \end{pmatrix}.\tag{B.2}$$

With these γ_i and γ_c , we define the gamma matrices for the two-coupled system $\Gamma_i^{(a)} = \sqrt{2} \psi_i^{(a)}$ ($a = L, R$) as

$$\Gamma_i^{(L)} = \gamma_i \otimes 1, \quad \Gamma_i^{(R)} = \gamma_c \otimes \gamma_i,\tag{B.3}$$

and define the fermion number parity matrix Γ_c for a two-coupled system as⁵

$$\Gamma_c = (-i)^N \Gamma_1^{(L)} \Gamma_2^{(L)} \cdots \Gamma_N^{(L)} \Gamma_1^{(R)} \Gamma_2^{(R)} \cdots \Gamma_N^{(R)} = \gamma_c \otimes \gamma_c.\tag{B.4}$$

Since $|I\rangle$, the ground state of H_{int} (2.2), satisfies $i\Gamma_i^{(L)}\Gamma_i^{(R)}|I\rangle = -|I\rangle$ for all $i = 1, 2, \dots, N$, we find that the fermion number parity of $|I\rangle$ is $\Gamma_c = (-1)^{\frac{N(N-1)}{2}}$.

The charge conjugation operator C of single site can be defined as

$$C = \gamma_2 \gamma_4 \cdots \gamma_N K,\tag{B.5}$$

⁵We have chosen the convention of Γ_c so that the fermion number of the two-coupled system always coincides with the sum of the fermion number of each site for any $N \in 2\mathbb{N}$. Note that our choice is different from the one $\Gamma_c^{(\text{another})} = (-4)^{\frac{N}{2}} \psi_1^{(L)} \psi_1^{(R)} \psi_2^{(L)} \psi_2^{(R)} \cdots \psi_N^{(L)} \psi_N^{(R)}$ with which the fermion parity of $|I\rangle$ is independent of N : $\Gamma_c^{(\text{another})}|I\rangle = |I\rangle$.

where K is the complex conjugation in the basis which define the matrix element of X, Y, Z as (B.2). Note that $CK = \gamma_2\gamma_4 \cdots \gamma_N$ is a unitary operator but C is not a unitary operator. Let us list several important properties of C :

$$C\gamma_i = (-1)^{\frac{N}{2}}\gamma_i C, \quad C\gamma_c = (-1)^{\frac{N}{2}}\gamma_c C, \quad C^2 = \begin{cases} 1 & (N = 0, 6 \bmod 8) \\ -1 & (N = 2, 4 \bmod 8) \end{cases}, \quad (\text{B.6})$$

$$\langle \phi | \gamma_i | \psi \rangle = (-1)^{\frac{N}{2}} (C|\psi\rangle)^\dagger \gamma_i C|\phi\rangle, \quad (\text{B.7})$$

which we use in the rest of this section.

B.2 $q = 0 \bmod 4$

For $q = 0 \bmod 4$, $H_{SYK}^{(L)}$ and $H_{SYK}^{(R)}$ with $J_{i_1 \dots i_q}^{(L)} = J_{i_1 \dots i_q}^{(R)}$ are written in the basis (B.3) as

$$H_{SYK}^{(L)} = H_{SYK} \otimes 1, \quad H_{SYK}^{(R)} = 1 \otimes H_{SYK}, \quad (\text{B.8})$$

with

$$H_{SYK} = \frac{1}{2^{\frac{q}{2}}} i^{\frac{q}{2}} \sum_{i_1 < \dots < i_q} J_{i_1 \dots i_q}^{(L)} \gamma_{i_1} \cdots \gamma_{i_q}. \quad (\text{B.9})$$

Since H_{SYK} commutes with γ_c , we can choose the eigenstates of H_{SYK} as simultaneous eigenstates of γ_c . Also, since H_{SYK} commutes with C , we can classify these eigenstates by using C . As the relations (B.6) suggest, the classification, as well as the consequent expression of $|I\rangle$, depends on $N \bmod 8$.

B.2.1 $q = 0 \bmod 4$, $N = 0 \bmod 8$

First let us consider the case $q = 0 \bmod 4$ and $N = 0 \bmod 8$. In this case γ_c and C also commute with each other. Therefore, if $|n, \sigma\rangle$ is an eigenstate of H_{SYK} with $H_{SYK} = E_{n, \sigma}$ and $\gamma_c = \sigma$, $C|n, \sigma\rangle$ is also an eigenstate of H_{SYK}, γ_c with $H_{SYK} = E_{n, \sigma}$ and $\gamma_c = \sigma$. Moreover, since $C^2 = 1$, we can choose the eigenstates $|n, \sigma\rangle$ such that $C|n, \sigma\rangle = |n, \sigma\rangle$: if $C|n, \sigma\rangle \neq |n, \sigma\rangle$ we can redefine $(|n, \sigma\rangle + C|n, \sigma\rangle) \times (\text{real number})$ and/or $i(|n, \sigma\rangle - C|n, \sigma\rangle) \times (\text{real number})$ as $|n, \sigma\rangle$. It turns out that there are no degeneracy with generic $J_{i_1 \dots i_q}^{(L)}$, hence the eigenstates of H_{SYK} are summarized as

| eigenstates of H_{SYK} | | γ_c | H_{SYK} | |
|--------------------------|--|------------|------------|---|
| $ n, +\rangle$ | $(C n, +\rangle = n, +\rangle; n = 1, 2, \dots, 2^{N/2-1})$ | +1 | $E_{n, +}$ | , (B.10) |
| $ n, -\rangle$ | $(C n, +\rangle = n, -\rangle; n = 1, 2, \dots, 2^{N/2-1})$ | -1 | $E_{n, -}$ | |

where $E_{n,+} \neq E_{n,-}$.

Since $|I\rangle$ satisfies $\Gamma_i^{(R)}|I\rangle = i\Gamma_i^{(L)}|I\rangle$, we have $H_{SYK}^{(L)}|I\rangle = H_{SYK}^{(R)}|I\rangle$, which suggests that $|I\rangle$ is expanded as

$$|I\rangle = \sum_{n=1}^{2^{N/2}-1} \sum_{\sigma=\pm 1} a_{n,\sigma} |n, \sigma\rangle \otimes |n, \sigma\rangle. \quad (\text{B.11})$$

Since the ground state of H_{int} is non-degenerate, $a_{n,\sigma}$ can be determined uniquely by solving $\langle I|H_{int}|I\rangle = -\frac{N}{2}$. By using the explicit expressions of $\Gamma_i^{(L)}, \Gamma_i^{(R)}$ (B.3) and the properties of $|n, \sigma\rangle$ under C, γ_c we can rewrite $\langle I|H_{int}|I\rangle$ as

$$\begin{aligned} \langle I|H_{int}|I\rangle &= \frac{i}{2} \sum_{i=1}^N \sum_{m,n} \sum_{\sigma} a_{m,\sigma}^* a_{n,-\sigma} \langle m, \sigma | \gamma_i \gamma_c | n, -\sigma \rangle \langle m, \sigma | \gamma_i | n, -\sigma \rangle \\ &= \frac{i}{2} \sum_{i=1}^N \sum_{m,n} \sum_{\sigma} (-\sigma) a_{m,\sigma}^* a_{n,-\sigma} \langle m, \sigma | \gamma_i | n, -\sigma \rangle \langle m, \sigma | \gamma_i | n, -\sigma \rangle \\ &= \frac{i}{2} \sum_{i=1}^N \sum_{m,n} \sum_{\sigma} (-\sigma) a_{m,\sigma}^* a_{n,-\sigma} \langle m, \sigma | \gamma_i | n, -\sigma \rangle \langle n, -\sigma | \gamma_i | m, \sigma \rangle, \end{aligned} \quad (\text{B.12})$$

where in the first line we have used the fact that γ_i flip the fermion number parity γ_c and in the third line we have used the formula (B.7). If we assume $a_{n,\sigma} = a_\sigma$ is independent of n , we can use the fact that $\{|n, \sigma\rangle\}$ is a complete orthonormal basis, i.e., $\sum_{n,\sigma'} |n, \sigma'\rangle \langle n, \sigma'| = 1$, to further simplify the right-hand side of (B.12):

$$\langle I|H_{int}|I\rangle = \frac{i}{2} \sum_{i=1}^N \sum_m \sum_{\sigma} (-\sigma) a_\sigma^* a_{-\sigma} \langle m, \sigma | \gamma_i \gamma_i | m, \sigma \rangle = -2^{N/2-2} i N \sum_{\sigma=\pm 1} \sigma a_\sigma^* a_{-\sigma}. \quad (\text{B.13})$$

Hence from $\langle I|H_{int}|I\rangle = -\frac{N}{2}$ we obtain the condition $2^{N/2-1} \sum_{\sigma} \sigma a_\sigma^* a_{-\sigma} = -i$. Combining this with the normalization condition $\langle I|I\rangle = 2^{N/2-1} \sum_{\sigma} |a_\sigma|^2 = 1$, we can determine a_σ as $(a_+, a_-) = (2^{-N/4}, -2^{-N/4}i)$ up to an overall phase. After all, we obtain the following expression for $|I\rangle$:

$$|I\rangle_{q=0 \bmod 4, N=0 \bmod 8} = 2^{-\frac{N}{4}} \sum_{n=1}^{2^{\frac{N}{2}-1}} (|n, +\rangle \otimes |n, +\rangle - i |n, -\rangle \otimes |n, -\rangle). \quad (\text{B.14})$$

B.2.2 $q = 0 \bmod 4, N = 2, 6 \bmod 8$

In this case γ_c anti-commutes with C . Hence if $|n, +\rangle$ is an eigenstate of H_{SYK} with $H_{SYK} = E_n$ and $\gamma_c = +1$, $C|n, +\rangle$ is another eigenstate of H_{SYK}, γ_c with $H_{SYK} = E_n$ and $\gamma_c = -1$, i.e., the

spectrum is degenerate between $\gamma_c = \pm 1$ sectors and summarized as follows

| eigenstates of H_{SYK} | γ_c | H_{SYK} |
|--|------------|-----------|
| $ n, +\rangle \quad (n = 1, 2, \dots, 2^{N/2-1})$ | +1 | E_n |
| $C n, +\rangle \quad (n = 1, 2, \dots, 2^{N/2-1})$ | -1 | E_n |

(B.15)

Taking into account the fact that $H_{SYK}^{(L)}|I\rangle = H_{SYK}^{(R)}|I\rangle$ together with the two-site parity $\Gamma_c|I\rangle = -|I\rangle$, we pose the following ansatz:

$$|I\rangle = \sum_{n=1}^{2^{N/2-1}} (a_{n,+}|n, +\rangle \otimes C|n, +\rangle + a_{n,-}C|n, +\rangle \otimes |n, +\rangle), \quad (B.16)$$

where we have defined $|n, -\rangle = C|n, +\rangle$. By imposing $\langle I|H_{int}|I\rangle = -\frac{N}{2}$ and $\langle I|I\rangle = 1$ we can determine $a_{n,\sigma}$ and obtain the following expressions:

$$\begin{aligned} |I\rangle_{q=0 \bmod 4, N=2 \bmod 8} &= 2^{-\frac{N}{4}} \sum_{n=1}^{2^{\frac{N}{2}-1}} (|n, +\rangle \otimes C|n, +\rangle - iC|n, +\rangle \otimes |n, +\rangle), \\ |I\rangle_{q=0 \bmod 4, N=6 \bmod 8} &= 2^{-\frac{N}{4}} \sum_{n=1}^{2^{\frac{N}{2}-1}} (|n, +\rangle \otimes C|n, +\rangle + iC|n, +\rangle \otimes |n, +\rangle). \end{aligned} \quad (B.17)$$

B.2.3 $q = 0 \bmod 4$, $N = 4 \bmod 8$

In this case γ_c commutes with C , hence $|n, \sigma\rangle$ and $C|n, \sigma\rangle$ have the same eigenvalues both for H_{SYK} and γ_c . In contrast to the case $N = 0 \bmod 8$, since $C^2 = -1$ it is impossible to have a state $|\phi\rangle$ as $C|\phi\rangle = |\phi\rangle$. This implies that there are two-fold degeneracy within each of $\gamma_c = \pm 1$ sector. In summary,

| eigenstates of H_{SYK} | γ_c | H_{SYK} |
|--|------------|-----------|
| $ n, +\rangle \quad (n = 1, 2, \dots, 2^{N/2-2})$ | +1 | $E_{n,+}$ |
| $C n, +\rangle \quad (n = 1, 2, \dots, 2^{N/2-2})$ | +1 | $E_{n,+}$ |
| $ n, -\rangle \quad (n = 1, 2, \dots, 2^{N/2-2})$ | -1 | $E_{n,-}$ |
| $C n, -\rangle \quad (n = 1, 2, \dots, 2^{N/2-2})$ | -1 | $E_{n,-}$ |

(B.18)

Taking into account $H_{SYK}^{(L)}|I\rangle = H_{SYK}^{(R)}|I\rangle$ and $\Gamma_c|I\rangle = |I\rangle$, we pose the following ansatz for $|I\rangle$:

$$\begin{aligned} |I\rangle &= \sum_{n=1}^{2^{N/2-2}} \sum_{\sigma=\pm} (a_{n,\sigma}|n, \sigma\rangle \otimes |n, \sigma\rangle + b_{n,\sigma}|n, \sigma\rangle \otimes C|n, \sigma\rangle + c_{n,\sigma}C|n, \sigma\rangle \otimes |n, \sigma\rangle + d_{n,\sigma}C|n, \sigma\rangle \otimes C|n, \sigma\rangle). \end{aligned} \quad (B.19)$$

By imposing $\langle I|H_{int}|I\rangle = -\frac{N}{2}$ and $\langle I|I\rangle = 1$ we can determine $a_{n,\sigma}, b_{n,\sigma}, c_{n,\sigma}, d_{n,\sigma}$ and obtain the following expression:

$$\begin{aligned}
& |I\rangle_{q=0 \bmod 4, N=4 \bmod 8} \\
&= 2^{-\frac{N}{4}} \sum_{n=1}^{2^{\frac{N}{2}-2}} \left(|n, +\rangle \otimes C|n, +\rangle - C|n, +\rangle \otimes |n, +\rangle - i(|n, -\rangle \otimes C|n, -\rangle - C|n, -\rangle \otimes |n, -\rangle) \right).
\end{aligned} \tag{B.20}$$

B.3 $q = 2 \bmod 4$

For $q = 2 \bmod 4$, $H_{SYK}^{(L)}$ and $H_{SYK}^{(R)}$ with $J_{i_1 \dots i_q}^{(L)} = J_{i_1 \dots i_q}^{(R)}$ are written in the basis (B.3) as

$$H_{SYK}^{(L)} = H_{SYK} \otimes 1, \quad H_{SYK}^{(R)} = -1 \otimes H_{SYK}, \tag{B.21}$$

with

$$H_{SYK} = \frac{1}{2^{\frac{q}{2}}} i^{\frac{q}{2}} \sum_{i_1 < \dots < i_q} J_{i_1 \dots i_q}^{(L)} \gamma_{i_1} \dots \gamma_{i_q}. \tag{B.22}$$

For $q = 2 \bmod 4$, H_{SYK} does not commute with C due to the factor $i^{\frac{q}{2}}$. Nevertheless, since H_{SYK} anti-commutes with C , an eigenstate of H_{SYK} with eigenvalue E_n transforms to another eigenstate of H_{SYK} with eigenvalue $-E_n$ and C is still useful to classify the eigenstates of H_{SYK} .

B.3.1 $q = 2 \bmod 4$, $N = 0, 4 \bmod 8$

Since γ_c and C commutes, we obtain the following classification of the spectrum of single H_{SYK} :

| eigenstates of H_{SYK} | γ_c | H_{SYK} |
|--|------------|------------|
| $ n, +\rangle \quad (n = 1, 2, \dots, 2^{N/2-2})$ | +1 | $E_{n,+}$ |
| $C n, +\rangle \quad (n = 1, 2, \dots, 2^{N/2-2})$ | +1 | $-E_{n,+}$ |
| $ n, -\rangle \quad (n = 1, 2, \dots, 2^{N/2-2})$ | -1 | $E_{n,-}$ |
| $C n, -\rangle \quad (n = 1, 2, \dots, 2^{N/2-2})$ | -1 | $-E_{n,-}$ |

(B.23)

There are no degeneracy for generic $J_{i_1 \dots i_q}^{(L)}$.

To write down an ansatz for $|I\rangle$ notice that $i\Gamma_i^{(L)}\Gamma_i^{(R)}|I\rangle = |I\rangle$ implies $(H_{SYK} \otimes 1)|I\rangle = -(1 \otimes H_{SYK})|I\rangle$ for $q = 2 \bmod 4$. Hence we need to pair an energy eigenstate of single site

with $H_{SYK} = E$ and a different energy eigenstate with $H_{SYK} = -E$. Taking this into account together with the classification (B.23) we pose the following ansatz:

$$|I\rangle = \sum_{n=1}^{2^{\frac{N}{2}-2}} \sum_{\sigma} (a_{n,\sigma} |n, +\rangle \otimes C|n, \sigma\rangle + b_{n,\sigma} C|n, \sigma\rangle \otimes |n, \sigma\rangle). \quad (\text{B.24})$$

Now we can determine the coefficients $a_{m,\sigma}, b_{m,\sigma}$ by completely the same strategy as we have used for $q = 4$, and we obtain

$$\begin{aligned} & |I\rangle_{q=2 \bmod 4, N=0 \bmod 8} \\ &= 2^{-\frac{N}{4}} \sum_{n=1}^{2^{\frac{N}{2}-2}} \left(|n, +\rangle \otimes C|n, +\rangle + C|n, +\rangle \otimes |n, +\rangle - i(|n, -\rangle \otimes C|n, -\rangle + C|n, -\rangle \otimes |n, -\rangle) \right), \\ & |I\rangle_{q=2 \bmod 4, N=4 \bmod 8} \\ &= 2^{-\frac{N}{4}} \sum_{n=1}^{2^{\frac{N}{2}-2}} \left(|n, +\rangle \otimes C|n, +\rangle - C|n, +\rangle \otimes |n, +\rangle - i(|n, -\rangle \otimes C|n, -\rangle - C|n, -\rangle \otimes |n, -\rangle) \right). \end{aligned} \quad (\text{B.25})$$

B.3.2 $q = 2 \bmod 4$, $N = 2, 6 \bmod 8$

Since γ_c and C anti-commutes, we obtain the following classification of the spectrum of single H_{SYK} :

| eigenstates of H_{SYK} | γ_c | H_{SYK} |
|--|------------|-----------|
| $ n, +\rangle \quad (n = 1, 2, \dots, 2^{N/2-1})$ | +1 | E_n |
| $C n, +\rangle \quad (n = 1, 2, \dots, 2^{N/2-1})$ | -1 | $-E_n$ |

(B.26)

There are no degeneracy for generic $J_{i_1 \dots i_q}^{(L)}$.

By posing the following ansatz

$$|I\rangle = \sum_{n=1}^{2^{\frac{N}{2}-1}} (a_{n,+} |n, +\rangle \otimes C|n, +\rangle + a_{n,-} C|n, +\rangle \otimes |n, +\rangle), \quad (\text{B.27})$$

we can obtain $|I\rangle$ as

$$\begin{aligned} |I\rangle_{q=2 \bmod 4, N=2 \bmod 8} &= 2^{-\frac{N}{4}} \sum_{n=1}^{2^{\frac{N}{2}-1}} (|n, +\rangle \otimes C|n, +\rangle - iC|n, +\rangle \otimes |n, +\rangle), \\ |I\rangle_{q=2 \bmod 4, N=6 \bmod 8} &= 2^{-\frac{N}{4}} \sum_{n=1}^{2^{\frac{N}{2}-1}} (|n, +\rangle \otimes C|n, +\rangle + iC|n, +\rangle \otimes |n, +\rangle). \end{aligned} \quad (\text{B.28})$$

References

- [1] S. Sachdev and J. Ye, “Gapless spin-fluid ground state in a random quantum heisenberg magnet,” Phys. Rev. Lett. **70** (May, 1993) 3339–3342.
<https://link.aps.org/doi/10.1103/PhysRevLett.70.3339>.
- [2] A. Kitaev, “A simple model of quantum holography,” talk at KITP strings seminar and Entanglement 2015 program (2015) .
<http://online.kitp.ucsb.edu/online/entangled15/>.
- [3] J. Maldacena, D. Stanford, and Z. Yang, “Conformal symmetry and its breaking in two dimensional Nearly Anti-de-Sitter space,” PTEP **2016** no. 12, (2016) 12C104, [arXiv:1606.01857 \[hep-th\]](#).
- [4] W. Israel, “Thermo field dynamics of black holes,” Phys. Lett. A **57** (1976) 107–110.
- [5] J. M. Maldacena, “Eternal black holes in anti-de Sitter,” JHEP **04** (2003) 021, [arXiv:hep-th/0106112](#).
- [6] M. Van Raamsdonk, “Building up spacetime with quantum entanglement,” Gen. Rel. Grav. **42** (2010) 2323–2329, [arXiv:1005.3035 \[hep-th\]](#).
- [7] S. Ryu and T. Takayanagi, “Holographic derivation of entanglement entropy from AdS/CFT,” Phys. Rev. Lett. **96** (2006) 181602, [arXiv:hep-th/0603001](#).
- [8] V. E. Hubeny, M. Rangamani, and T. Takayanagi, “A Covariant holographic entanglement entropy proposal,” JHEP **07** (2007) 062, [arXiv:0705.0016 \[hep-th\]](#).
- [9] N. Engelhardt and A. C. Wall, “Quantum Extremal Surfaces: Holographic Entanglement Entropy beyond the Classical Regime,” JHEP **01** (2015) 073, [arXiv:1408.3203 \[hep-th\]](#).
- [10] J. Maldacena and L. Susskind, “Cool horizons for entangled black holes,” Fortsch. Phys. **61** (2013) 781–811, [arXiv:1306.0533 \[hep-th\]](#).
- [11] B. Swingle, “Constructing holographic spacetimes using entanglement renormalization,” [arXiv:1209.3304 \[hep-th\]](#).
- [12] S. R. Coleman, “Black Holes as Red Herrings: Topological Fluctuations and the Loss of Quantum Coherence,” Nucl. Phys. B **307** (1988) 867–882.
- [13] S. B. Giddings and A. Strominger, “Loss of Incoherence and Determination of Coupling Constants in Quantum Gravity,” Nucl. Phys. B **307** (1988) 854–866.

- [14] S. B. Giddings and A. Strominger, “Axion Induced Topology Change in Quantum Gravity and String Theory,” Nucl. Phys. B **306** (1988) 890–907.
- [15] P. Saad, S. H. Shenker, D. Stanford, and S. Yao, “Wormholes without averaging,” [arXiv:2103.16754 \[hep-th\]](#).
- [16] P. Saad, S. Shenker, and S. Yao, “Comments on wormholes and factorization,” [arXiv:2107.13130 \[hep-th\]](#).
- [17] A. Almheiri, T. Hartman, J. Maldacena, E. Shaghoulian, and A. Tajdini, “Replica Wormholes and the Entropy of Hawking Radiation,” JHEP **05** (2020) 013, [arXiv:1911.12333 \[hep-th\]](#).
- [18] G. Penington, S. H. Shenker, D. Stanford, and Z. Yang, “Replica wormholes and the black hole interior,” [arXiv:1911.11977 \[hep-th\]](#).
- [19] D. Bak, M. Gutperle, and S. Hirano, “Three dimensional Janus and time-dependent black holes,” JHEP **02** (2007) 068, [arXiv:hep-th/0701108](#).
- [20] D. Bak, M. Gutperle, and R. A. Janik, “Janus Black Holes,” JHEP **10** (2011) 056, [arXiv:1109.2736 \[hep-th\]](#).
- [21] Y. Nakaguchi, N. Ogawa, and T. Ugajin, “Holographic Entanglement and Causal Shadow in Time-Dependent Janus Black Hole,” JHEP **07** (2015) 080, [arXiv:1412.8600 \[hep-th\]](#).
- [22] A. Goel, H. T. Lam, G. J. Turiaci, and H. Verlinde, “Expanding the Black Hole Interior: Partially Entangled Thermal States in SYK,” [arXiv:1807.03916 \[hep-th\]](#).
- [23] D. Bak, M. Gutperle, and A. Karch, “Time dependent black holes and thermal equilibration,” JHEP **12** (2007) 034, [arXiv:0708.3691 \[hep-th\]](#).
- [24] J. Maldacena and X.-L. Qi, “Eternal traversable wormhole,” [arXiv:1804.00491 \[hep-th\]](#).
- [25] P. Gao, D. L. Jafferis, and A. C. Wall, “Traversable Wormholes via a Double Trace Deformation,” JHEP **12** (2017) 151, [arXiv:1608.05687 \[hep-th\]](#).
- [26] P. Gao and H. Liu, “Regenesi and quantum traversable wormholes,” JHEP **10** (2019) 048, [arXiv:1810.01444 \[hep-th\]](#).

- [27] A. M. García-García, T. Nosaka, D. Rosa, and J. J. M. Verbaarschot, “Quantum chaos transition in a two-site Sachdev-Ye-Kitaev model dual to an eternal traversable wormhole,” Phys. Rev. **D100** no. 2, (2019) 026002, [arXiv:1901.06031 \[hep-th\]](#).
- [28] F. Alet, M. Hanada, A. Jevicki, and C. Peng, “Entanglement and Confinement in Coupled Quantum Systems,” JHEP **02** (2021) 034, [arXiv:2001.03158 \[hep-th\]](#).
- [29] T. Nosaka and T. Numasawa, “Quantum Chaos, Thermodynamics and Black Hole Microstates in the mass deformed SYK model,” [arXiv:1912.12302 \[hep-th\]](#).
- [30] T. Nosaka and T. Numasawa, “Chaos exponents of SYK traversable wormholes,” JHEP **02** (2021) 150, [arXiv:2009.10759 \[hep-th\]](#).
- [31] A. M. García-García, Y. Jia, D. Rosa, and J. J. M. Verbaarschot, “Dominance of Replica Off-Diagonal Configurations and Phase Transitions in a PT Symmetric Sachdev-Ye-Kitaev Model,” Phys. Rev. Lett. **128** no. 8, (2022) 081601, [arXiv:2102.06630 \[hep-th\]](#).
- [32] A. M. García-García, Y. Jia, D. Rosa, and J. J. M. Verbaarschot, “Replica Symmetry Breaking in Random Non-Hermitian Systems,” [arXiv:2203.13080 \[hep-th\]](#).
- [33] A. M. García-García, V. Godet, C. Yin, and J. P. Zheng, “Euclidean-to-Lorentzian wormhole transition and gravitational symmetry breaking in the Sachdev-Ye-Kitaev model,” [arXiv:2204.08558 \[hep-th\]](#).
- [34] N. Sorokhaibam, “Traversable wormhole without interaction,” [arXiv:2007.07169 \[hep-th\]](#).
- [35] W. Cai, S. Cao, X.-H. Ge, M. Matsumoto, and S.-J. Sin, “A Non-Hermitian two coupled Sachdev-Ye-Kitaev model,” [arXiv:2208.10800 \[hep-th\]](#).
- [36] I. Kourkoulou and J. Maldacena, “Pure states in the SYK model and nearly- AdS_2 gravity,” [arXiv:1707.02325 \[hep-th\]](#).
- [37] S. Plugge, E. Lantagne-Hurtubise, and M. Franz, “Revival dynamics in a traversable wormhole,” Phys. Rev. Lett. **124** no. 22, (2020) 221601, [arXiv:2003.03914 \[cond-mat.str-el\]](#).
- [38] A. I. Larkin and Y. N. Ovchinnikov, “Quasiclassical Method in the Theory of Superconductivity,” Soviet Journal of Experimental and Theoretical Physics **28** (Jun, 1969) 1200.

- [39] X.-L. Qi and P. Zhang, “The Coupled SYK model at Finite Temperature,” JHEP **05** (2020) 129, [arXiv:2003.03916 \[hep-th\]](#).
- [40] A. Almheiri and H. W. Lin, “The entanglement wedge of unknown couplings,” JHEP **08** (2022) 062, [arXiv:2111.06298 \[hep-th\]](#).
- [41] A. Streicher, “SYK Correlators for All Energies,” JHEP **02** (2020) 048, [arXiv:1911.10171 \[hep-th\]](#).
- [42] T. Kanazawa and T. Wettig, “Complete random matrix classification of SYK models with $\mathcal{N} = 0, 1$ and 2 supersymmetry,” JHEP **09** (2017) 050, [arXiv:1706.03044 \[hep-th\]](#).